energy&fuels

pubs.acs.org/EF

Review

Review on Template Removal Techniques for Synthesis of Mesoporous Silica Materials

Hosein Ghaedi and Ming Zhao*

Cite This: https://doi.org/10.1021/acs.energyfuels.1c04435

Read Online

ACCESS | Metrics & More | Article Recommendations

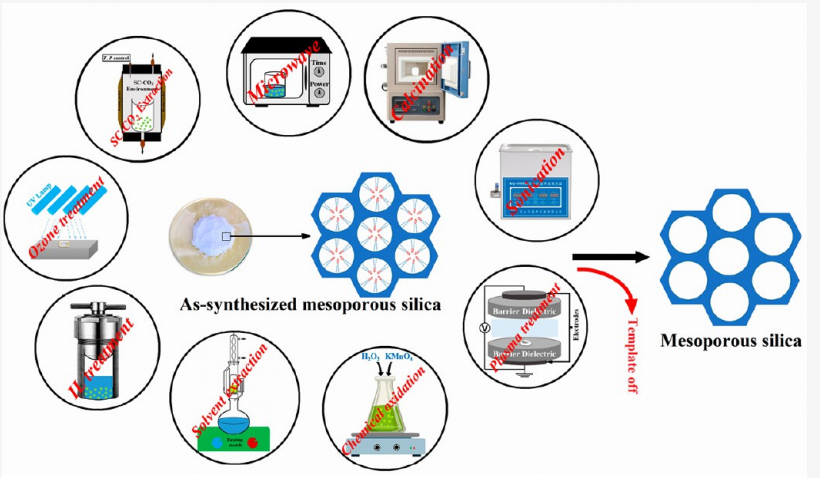

ABSTRACT: The key step in the preparation of mesoporous silica materials is the removal of organic templates occluded inside the pores including nonionic, cationic, anionic surfactants and even ionic liquid (IL). The most common method to remove templates is conventional calcination under air at 550 °C. Although templates can be completely removed from the pores, calcination suffers many serious drawbacks including significant framework shrinkage, the collapse of the ordered structure, reduction of silanol concentrations on the pore wall (which are of high importance for postmodification), generation of large amounts of CO_2 and organic amine compounds, the presence of carbon deposits or coke as a contaminant, elimination of organic functionalities (such as organoalkoxysilanes with amino groups), and the inability to recover or reuse expensive organic templates. That is why many attempts have been reported in the literature to develop novel methods for removing organic templates that are favorable from both economic and environmental standpoints for potentially large-scale applications. The current study reviews the recent development methods for template removal from various types of mesoporous silica materials. We have divided the template removal approaches into two categories: physical method and chemical method. The effects of those methods are discussed in detail on the textural and structural properties of mesoporous silica materials along with the template removal mechanism and their pores and coins.

1. INTRODUCTION

Mesoporous silica materials, for instance, the SBA (Santa Barbara Amorphous) series, MCM (Mobil Composition of Matter) series, and KIT (Korean Advanced Institute of Science and Technology) series have gained extensive attention over the last decades due to their highly tunable textural and chemical characteristics and are therefore used in different fields: biomedical and pharmaceutical applications,[1−3] adsorption of pollutants from wastewater,[4,5] catalysis,[6−9] aromatization,[10] biogas purification and upgrading,[11] sensing,[12] desulfurization,[13−20] for CO_2 capture,[21−27] Li-ion battery application,[28] upgrading microalgal biocrude,[29] hydrodenitrogenation,[30] and hydrogen production.[31,32] Figure 1(a) displays the number of publications for mesoporous silica materials, and Figure 1(b) shows their applications in different research areas from 2000 to 2021 (Web of Science). Poly(ethylene glycol)-*block*-poly(propylene glycol)-*block*-poly(ethylene glycol) (P123 copolymer), poly(ethylene oxide)-poly(propylene oxide)-poly(ethylene oxide) (pluronic F-127) as nonionic surfactants, cetyltrimethylammonium bromide

Received: December 30, 2021
Revised: January 28, 2022

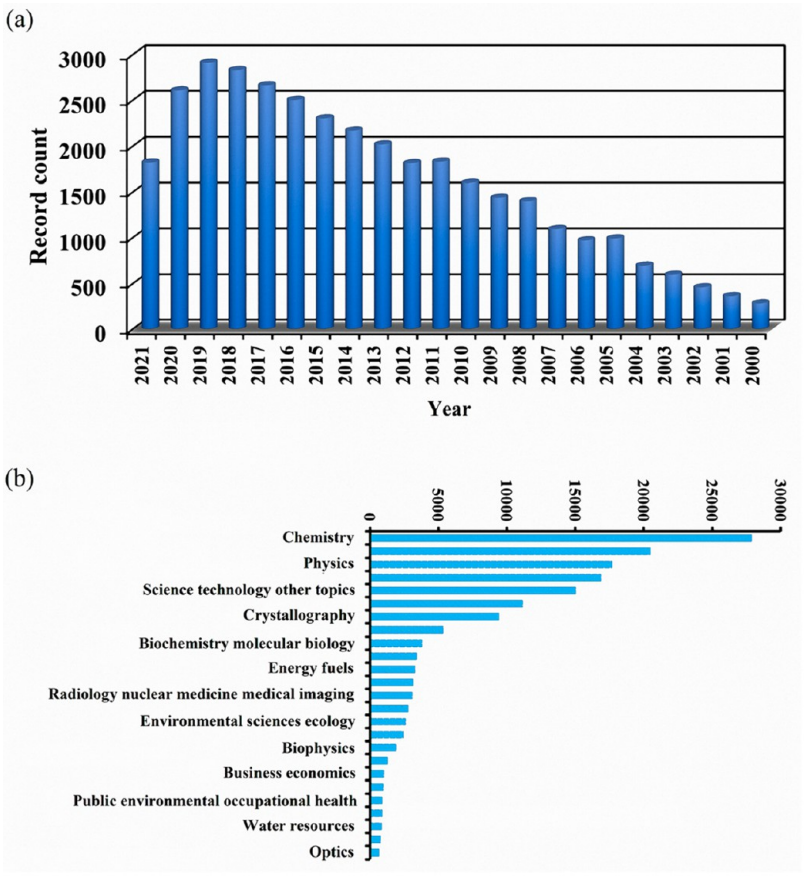

Figure 1. (a) Number of publications for mesoporous silica materials from 2000 to 2021. (b) Applications of mesoporous silica materials in different research fields published on the Web of Science with the keyword of "mesoporous silica material" (accessed December 25, 2021).

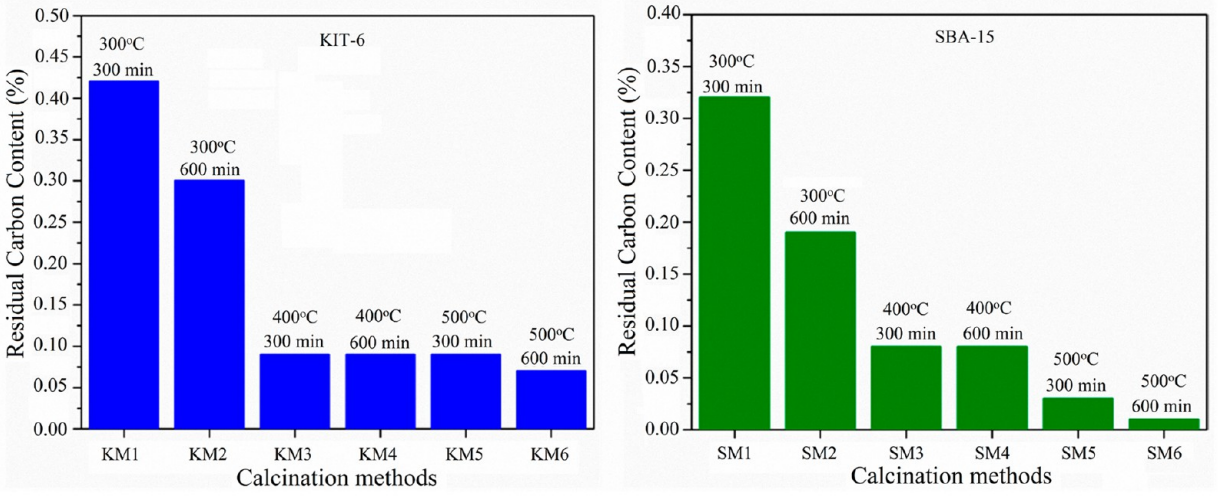

Figure 2. Residual carbon content for calcined SBA-15 and KIT-6 at various temperatures and times. Reproduced from ref 34. [Basso, A. M.; Nicola, B. P.; Bernardo-Gusmão, K.; Pergher, S. B. C. Tunable Effect of calcination of the silanol groups of KIT-6 and SBA-15 Mesoporous Materials. *Applied Sciences* **2020**, *10* (3), 970]. Copyright 2020, MDPI.

(CTABr), and cetyltriethylammonium bromide (CTEABr) as cationic surfactants, and anionic surfactants such as sodium dodecyl benzenesulfonate (SDBS) and sodium dodecyl sulfate (SDS) as well as ionic liquid (IL) are the common organic templates used for the synthesis of mesoporous silica materials. The elimination of these templates from the pores is a crucial step in the synthesis of mesoporous silica materials. Thermal calcination is a common method for template removal in the laboratory due to high efficiency, easy operation, and required simple equipment. The significant reduction of silanol concentrations happens during calcination (which renders the sample unsuitable for postmodification), and accordingly, the structural shrinkage is invariably detected following template removal. Also, the recovery or reuse of expensive templates is not possible due to burning out of the template which results in CO_2 and hazardous gas emissions that are

https://doi.org/10.1021/acs.energyfuels.1c04435
Energy Fuels XXXX, XXX, XXX−XXX

Table 1. Physical Properties of SBA-15 and KIT-6 in Ref 34

		S_{BET} (m^2 g^{-1})		Pore diameter (nm)		V_T (cm^3 g^{-1})		Wall thickness (nm)	
Temperature (°C)	Time (min)	SBA-15	KIT-6	SBA-15	KIT-6	SBA-15	KIT-6	SBA-15	KIT-6
300	300	572	695	7.5	7.2	0.79	0.82	4.5	15.8
300	600	632	826	7.5	6.1	0.86	0.98	4.4	17.9
400	300	641	905	7.8	7.5	0.84	1.07	4.7	16.0
400	600	1197	852	7.5	7.9	1.52	1.03	5.0	15.9
500	300	1099	1174	9.0	7.3	1.69	1.44	3.3	16.7
500	600	770	874	7.8	7.4	0.98	1.20	4.2	15.6

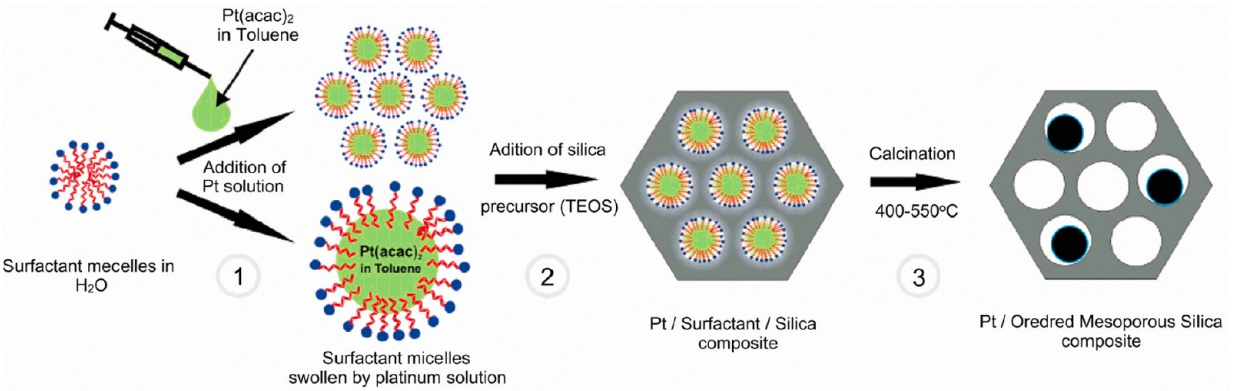

Figure 3. In situ preparation of Pt/mesoporous composite materials using catalytic template removal method. Reproduced from ref 37. [Krawiec, P.; Kockrick, E.; Simon, P.; Auffermann, G.; Kaskel, S. Platinum-Catalyzed Template Removal for the in Situ Synthesis of MCM-41 Supported Catalysts. *Chem. Mater.* **2006**, *18* (11), 2663−2669].Copyright 2006, American Chemical Society.

both economically and environmentally unfavorable. Furthermore, calcination burns off not only the template but also the functional groups when the mesoporous silica materials are modified via a co-condensation method with functional groups. Therefore, alternate detemplating procedures to calcination are needed, and more recent attention has focused on new technologies and methods offering superior template removal performance. To the best of our knowledge, this is the first study to review the latest developed methods for template removal including chemical methods such as solvent extraction, chemical oxidation, and ionic liquid (IL) treatment and physical methods such as calcination, supercritical CO_2 ($SC-CO_2$), microwave-assisted treatment, ultrasonic-assisted treatment, ozone treatment, and plasma technology. This review paves the way for researchers to get more information about these developed methods by weighing their benefits and drawbacks before developing and designing new template removal methods. Therefore, in this current study, the methods for the elimination of templates from mesoporous silica materials will be comprehensively reviewed, and finally a new, green, and efficient method will be proposed for template removal.

2. TEMPLATE REMOVAL APPROACHES

Several template removal methods have been reported in the literature. We have categorized these methods into physical and chemical methods. The physical methods are calcination, supercritical fluid, ozone treatment, microwave-assisted treatment, ultrasonic-assisted treatment, and plasma technology. The chemical methods are solvent extraction, chemical oxidation, and ionic liquid (IL) treatment.

2.1. Physical Methods. *2.1.1. Calcination.* Calcination in air is a common method and is widely used for template removal from pores.[33] Basso et al.[34] investigated the influence of calcination conditions (temperature and time) on the carbon content, silanol groups, and physical properties of SBA-15 and KIT-6. As shown in Figure 2, at 300 °C, the remaining carbon contents were 0.32% and 19% for SBA-15 and 0.42% and 0.30% for KIT-6 after 300 and 600 min, respectively. By increasing temperature to 400 and 500 °C, less of a difference in the amount of carbon was observed for both SBA-15 and KIT-6. Also, it can be seen that increasing the calcination time to 10 h at higher temperatures did not have a substantial effect on the removal of organic material. However, increasing the calcination period from 300 to 600 min resulted in a significant change in the carbon percent of SBA-15 at 300 °C, while residual carbon remained almost the same by increasing the calcination time from 300 to 600 min at a temperature more than 300 °C. Table 1 presents the physical properties of SBA-15 at various temperatures and times.

SBA-15 had the highest specific surface area (S_{BET}) at 400 °C calcination for 10 h. The S_{BET} decreased as the calcination temperature increased to 500 °C, even increasing calcination time at this temperature decreased slightly the S_{BET} of SBA-15 due to the dehydroxylation of the material. The pore diameter and total pore volume (V_T) followed the same trend, reaching their maximum values of 0.9 nm and 1.69 cm^3 g^{-1}, respectively, after 3000 min 500 °C. The highest wall thickness of 5.0 nm was at 400 °C for 600 min. Regarding KIT-6, the highest S_{BET} was obtained at 500 °C for 5 h, further increasing calcination time decreased its S_{BET}, as presented in Table 1. KIT-6 had the highest V_T and wall thickness at 500 °C for 5 h, while it has the highest pore diameter at the lower temperature of 400 °C for 10 h.

Moreover, by increasing the temperature, the conversion of geminal silanols has happened to siloxane. It was found that more silanol groups are preserved at 300 °C for 300 min rather than calcination at 400 °C. Nevertheless, calcination at 300 °C

https://doi.org/10.1021/acs.energyfuels.1c04435
Energy Fuels XXXX, XXX, XXX−XXX

Table 2. Elemental Analysis and Textural Properties of Calcined MCM-41 and H_2-Treated MCM-41 in Ref 40

Template removal method and condition	C (%)	H (%)	N (%)	S_{BET} (m^2 g^{-1})	V_T (cm^3 g^{-1})
H_2 flow treatment at 110 for 15 h	28.44	5.72	1.74	143	0.22
H_2 flow treatment at 150 for 15 h	22.25	4.55	1.49	282	0.29
H_2 flow treatment at 200 for 15 h	6.52	1.69	0.32	1006	0.95
H_2 flow treatment at 250 for 15 h	3.89	1.25	0.12	1169	1.10
Calcination in O_2 at 550 for 8 h	2.78	1.20	0.11	1126	1.07

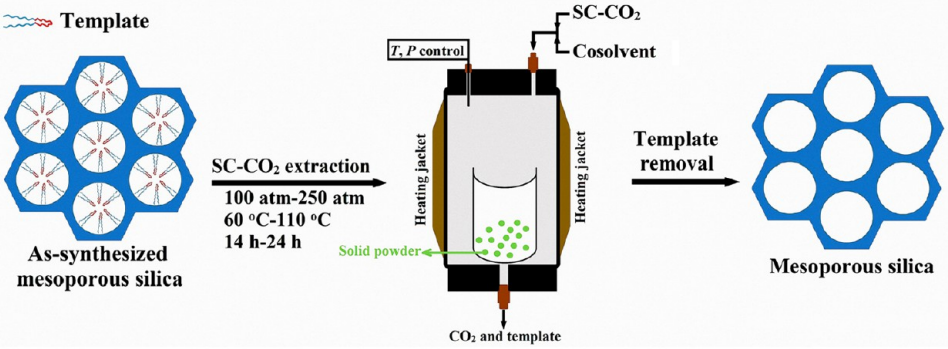

Figure 4. Schematic of SC−CO_2 extraction technique.

resulted in a small pore volume. It was suggested that calcination at a higher temperature, for example, 600 for 300 min, is unnecessary, time consuming, and a waste of silanol groups. Although the template is completely removed through calcination, there are some concerns with using this conventional method. The expensive organic template cannot be recovered after calcination. A high temperature and a long time are required to eliminate the template. During calcination, terrible smells, toxic and noxious gases, are produced leading to environmental pollution. Preserving large numbers of surface silanol groups is essential to functionalize the mesoporous siliceous materials for the desired application. During the calcination, the number of surface silanol groups reduces because of the dehydroxylation at higher temperatures for a prolonged time, and a significant structural shrinkage is observed resulting in the destruction of microporosity.[35,36] Moreover, calcination is not recommended if the material is functionalized with a less stable organic part because it might be eliminated together with the template.

Calcination was assisted by catalytic template treatment. Catalytic template removal is a fascinating technique in which metal acts as a catalyst for the oxidative elimination of the surfactant molecules during the calcination process. The calcination temperature in this process is less than the usual calcination temperature. The metals are injected in one step, as shown in Figure 3, or separately through impregnation. This technique has the benefit of lowering the calcination temperature substantially. This method was employed by Krawiec et al.[37] to prepare Pt/MC-41 and Pt/SBA-15. The calcination temperature and time were 450 °C and 5 h. They reported that Pt incorporation into SBA-15 pores was less successful in comparison to MCM-41 due to the long time required for the synthesis of SBA-15 (28 h). Indeed, during the long time synthesis, the diffusion of the metal precursor happened from the toluene to the mixture of ethanol−water resulting from TEOS hydrolysis. The surface area of sample 1 wt % Pt/SBA-15 was 825 m^2 g^{-1}, while that of of free metal SBA-15 was 786 m^2 g^{-1}. Other metals such as Pd and V_2O_5 have been used in this method.

The remaining trace of carbon after calcination is another disadvantage which is required further treatment, for example, in an oxygen (O_2) or hydrogen (H_2) stream to remove carbon on the silica surface.[38,39] Goworek et al.[40] have made efforts to remove surfactants from MCM-41 using H_2 flow treatment at the temperature range from 110 to 250 °C for 15 h. The elemental analysis showed that the amounts of hydrocarbon species and nitrogen compounds are significantly reduced by increasing temperature to 250 °C as presented in Table 2. According to data in Table 2, calcined MCM-41 in O_2 and MCM-41 treated in H_2 flow at 250 °C exhibited almost the same S_{BET} and V_T values. The pore size distribution curves of calcined and H_2-treated samples were quite narrow centered at 2.4 nm indicating high template removal efficiency of H_2 flow treatment. The ^{29}Si MAS NMR confirmed the high surface silanols content of MCM-41 treated in H_2 flow at 250 °C. The gas chromatography−mass spectrometry (GC-MS) analysis showed that the retention times of aliphatic hydrocarbons for both calcined and H_2 flow-treated MCM-41 are not identical due to differences in the surface properties of these materials. The collected products after H_2 flow treatment were condensed and analyzed by GC-MS. The peaks observed in GC-MS were assigned to hexadecane and hexadecane-*N*,*N*-dimethylamine indicating that the structures of surfactant molecules were damaged during the H_2 flow treatment only within the headgroup, and finally, the degradation products were evaporated. It was stated that the Hoffman degradation resulted in partial removal of amine groups and production of unsaturated product at a temperature below 250 °C. It might be possible to remove the remaining amount of amine compound in the MCM-41 skeleton through the burnoff process at high temperatures under oxidizing conditions. Although this method template can be removed at low temperatures, the deposition of carbon is more compared to calcination. Also, the removal time is long. The template cannot be recovered and reused, and a complex device is required.

2.1.2. Supercritical CO_2 (SC−CO_2) Extraction. Supercritical CO_2 (SC−CO_2) extraction is used not only for the synthesis of

https://doi.org/10.1021/acs.energyfuels.1c04435
Energy Fuels XXXX, XXX, XXX−XXX

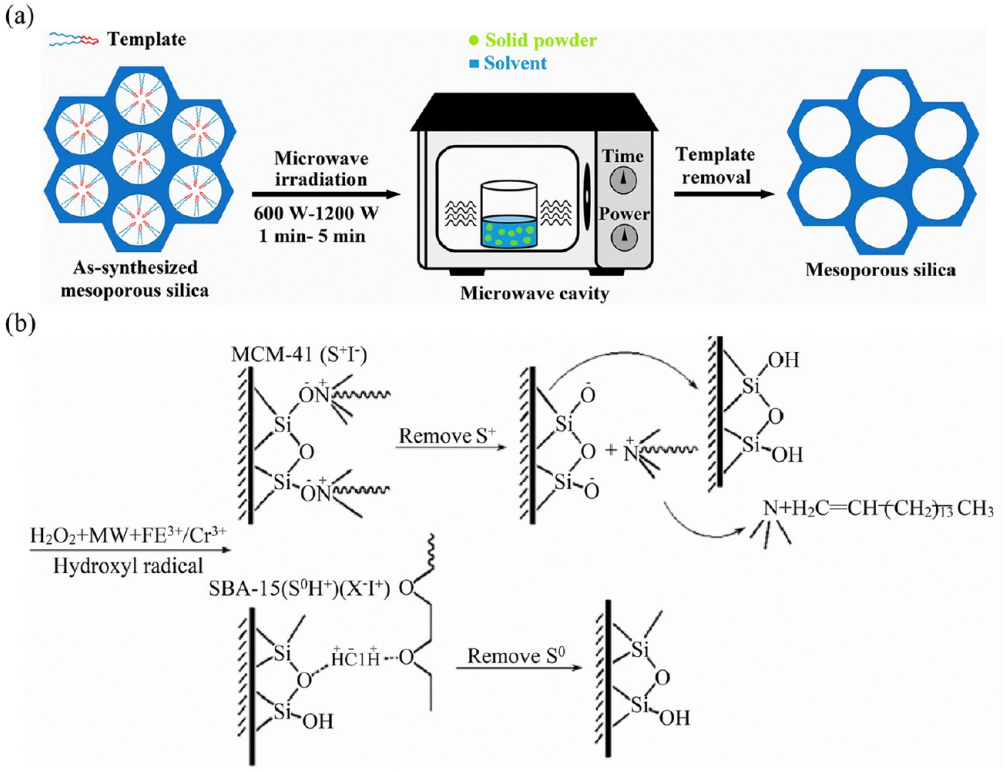

Figure 5. (a) Schematic of microwave-assisted treatment. (b) Possible mechanism for template removal from MCM-41 and SBA-15 using H_2O_2 treatment assisted by microwave. Reproduced from ref 48. [Chen, L.; Jiang, S.; Wang, R.; Zhang, Z.; Qiu, S. A novel, efficient and facile method for the template removal from mesoporous materials. *Chemical Research in Chinese Universities* **2014**, *30* (6), 894−899]. Copyright 2014, Springer.

adsorbent but also for template removal. The main advantage of this method is the adjustable physical and chemical properties including density, viscosity, diffusivity, and mass transfer by changing the operating pressure and temperature. For example, supercritical fluid (SCF) possesses high diffusivity and negligible surface tension, and penetration of solvent into cavities of mesoporous materials is rapid due to the gas-like viscosity of SFC. Since CO_2 as a special chemical with a low critical temperature of 304.21 K and modest critical pressure of 7.38 MPa is cost effective, available, low toxic, and nonflammable,[41,42] SC−CO_2 has attracted more attention of material scientists. SC−CO_2 in the presence or absence of cosolvents has been employed for template removal from mesoporous materials,[35,36,43−47] as shown in Figure 4. van Grieken et al.[45] extracted the nonionic surfactant from SBA-15 using SC−CO_2 in the presence and absence of ethanol as a cosolvent at various pressures and temperatures ranging from 60 to 110 °C for 24 h. The results disclosed that optimum removal efficiency of 79% is obtained upon using SC−CO_2 at 90 °C and 140 atm, while the efficiency is decreased to 76% by increasing temperature to 110 °C at 210 atm due to the lower density of the supercritical fluid. A higher extraction efficiency can be achieved using SC−CO_2 in comparison to the ethanol extraction method with a removal efficiency of 74%. The removal of the P123 copolymer from SBA-15 was enhanced by the addition of ethanol as a cosolvent so that removal efficiency increased to 81% at 90 °C and 130 atm. The silanol group concentration on the surface of SBA-15 was evaluated using ^{29}Si nuclear magnetic resonance (NMR) by obtaining a Q_3/Q_4 ratio. This ratio for calcined SBA-15 was 0.14, much lower than that of SBA-15 treated by SC−CO_2 in the absence and presence of ethanol having the values of 0.48 and 0.42, respectively. This result confirms that SC−CO_2 preserves more silanol groups on the surface of SBA-15 compared to calcination. Finding optimum experimental conditions is important which was not considered in the experimental conditions reported by van Grieken et al.[45] It seems that temperature, pressure, extraction time, and type of cosolvent (if used) and flow rates of liquid CO_2 and cosolvent (if used) are the main factors affecting the template removal efficiency, as reported in the literature.[35,43,46,47] When SC−CO_2 was employed without adding cosolvents, the cationic surfactant was not removed from MCM-41,[44] while van Grieken et al.[45] observed that SC−CO_2 alone was successful in removing the P123 copolymer from SBA-15 with a high removal efficiency, despite the extended reaction time (24 h).

The extracted organic template can be recovered and reused at the end of the process. It should be mentioned again that adding cosolvent can increase the template removal efficiency compared to SC−CO_2 alone because adding cosolvents can improve the solvating strength of SC−CO_2. The supercritical conditions can facilitate the transfer and desorption of templates through the inner and outer diffusion in the mesopores of materials due to SC−CO_2's low viscosity and high diffusivity properties. Huang and co-workers[35,36] used methanol-modified SC−CO_2 to extract cationic surfactant templates such as CTABr from MCM-41, MCM-48, and SBA-3 and cetyltriethylammonium bromide (CTEABr) from SBA-1. Their results showed the highest template removal efficiency of 95% for as-synthesized SBA-3 followed by as-synthesized MCM-48, SBA-1, and MCM-41 with efficiencies of 93%, 88%, and 78%, respectively. However, the destruction of the mesoporous framework of as-synthesized MCM-48 happened after template removal. They employed a curing treatment

https://doi.org/10.1021/acs.energyfuels.1c04435
Energy Fuels XXXX, XXX, XXX−XXX

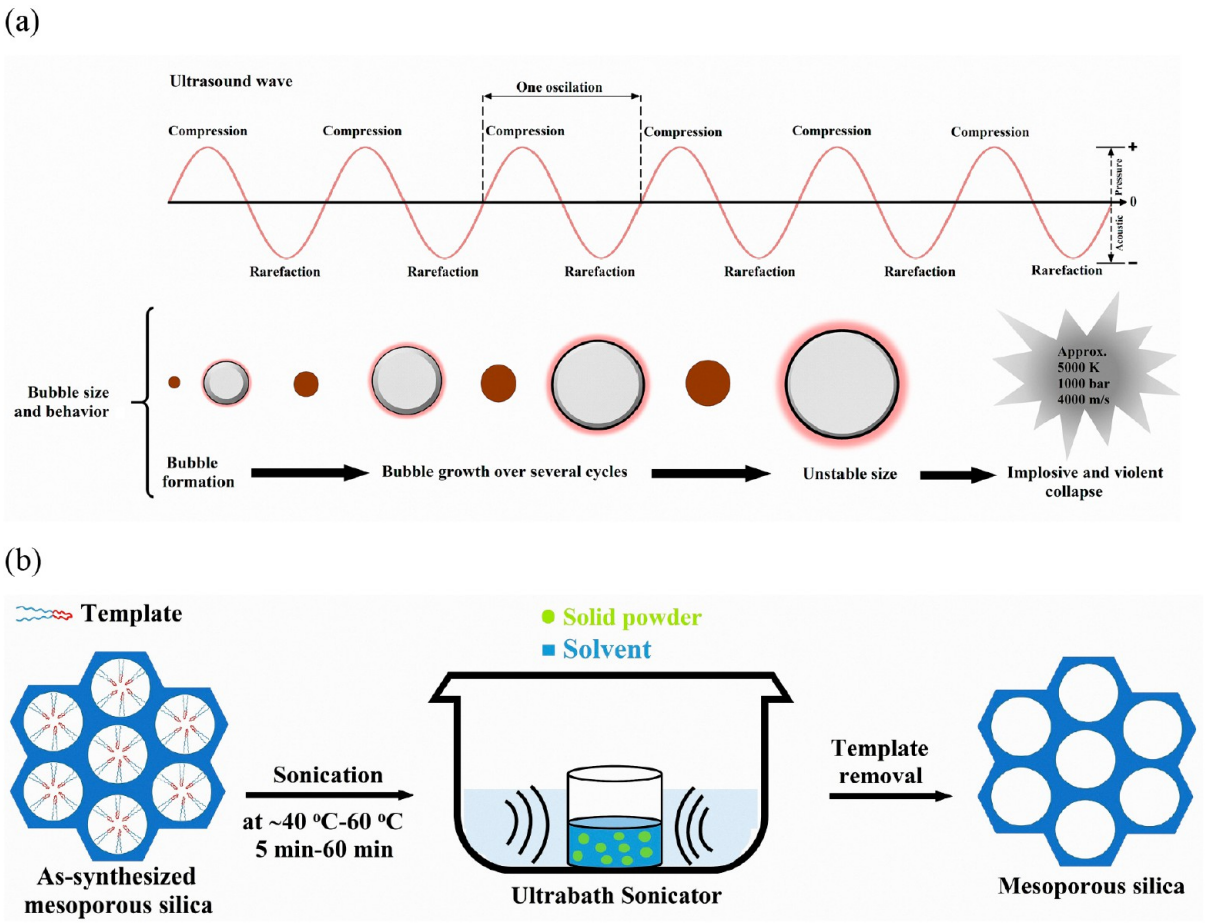

Figure 6. (a) Generation of acoustic bubbles by ultrasonic irradiation. (b) Schematic of ultrasonic-assisted treatment.

under vacuum for 14 h to improve the mesoporous structural stability of materials. Although cured as-synthesized materials had better ordered mesoporous structures and were stable after template removal, the template removal efficiency was reduced. Overall, it is not easy to carry out SC−CO_2 because of equipment limitations and difficulty in achieving the appropriate temperature, pressure, and CO_2 flow speed.[48]

2.1.3. Microwave-Assisted Treatment. Figure 5(a) illustrates a schematic of microwave-assisted treatment. Tian et al.[49] used microwave digestion to remove the template from SBA-15 and MCM-41. The sample was mixed with nitric acid (HNO_3) and hydrogen peroxide (H_2O_2) and placed in a reactor. These chemicals are utilized in the chemical oxidation process for template removal, which is discussed later. The oxidation of the template by HNO_3 and H_2O_2 is facilitated by the instantaneous high temperature (~200 °C) and pressure (~1.3 MPa) created by microwave radiation. The template in SBA-15 was completely removed within 2−3 min and confirmed by Fourier transform infrared spectroscopy (FT-IR) results. Also, the relative intensity of Si−OH bending bands at around 960 cm^{-1} was higher for SBA-15 treated by this method than calcined SBA-15. It suggests that microwave digestion-assisted treatment can preserve more silanol groups on the pore wall surface in comparison to calcination. Lai et al.[50] used microwave-assisted treatment to eliminate the template from the pores of as-synthesized SBA-15. The sample was mixed with 20 mL of ethanol/hexane (V/V, 1/1) as extract solvents and put on a watch glass, then heated for 2 min by microwave irradiation. The process for template removal was repeated three times. The obtained results were the same as those reported by Tian et al.[49] suggesting the effectiveness of this method in template removal. Chen et al.[48] used a combination of H_2O_2 treatment and a microwave to eliminate the template from SBA-15 and MCM-41. The process was catalyzed by Fe $(NO_3)_3{\cdot}9H_2O$ or Cr $(NO_3)_3{\cdot}9H_2O$ based on the Fenton reaction. Their results showed that the *d*-spacing values and the unit cell parameters (a_0) of SBA-15 and MCM-41 treated by this method were the same as the as-synthesized samples, while larger than those of the calcined SBA-15 and MCM-41 demonstrating that the shrinkage of the textural framework was significantly reduced using this method compared to calcination. As Fe $(NO_3)_3{\cdot}9H_2O$ was used as a Fenton reagent, SBA-15 has better pore properties. However, MCM-41 exhibited better textural parameters as Cr $(NO_3)_3{\cdot}9H_2O$ was used as Fenton reagent. Figure 5(b) shows the proposed mechanism for template removal. There was a stronger interaction between Fe(III) and anionic silicate species (I^-) due to higher coordination ability Fe(III) compared to Cr(III); therefore, removal of the cationic surfactant (S^+) from the MCM-41 system was not efficient. Moreover, trimethylamine species were produced by the decomposition of cationic surfactant CTABr (S^+I^-) resulting in the activity loss of Fe(III) and Cr(III). That is why the cationic template was removed from MCM-41 in the presence of the Cr−H_2O_2 reagent. The H^+ groups were significant in the removal of nonionic surfactant (S^0) from SBA-15 in, as well as

https://doi.org/10.1021/acs.energyfuels.1c04435
Energy Fuels XXXX, XXX, XXX−XXX

Table 3. Template Removal from SBA-15 and $PrSO_3$-SBA-15 in Ref 62[a]

Template removal method	Solvent	Time (h or min)	Solvent:Sample ($cm^3\ g^{-1}$)	Template removed (%)
		SBA-15		
Calcination	–	–	–	98
	Toluene	24 h	500	35
Reflux	Tetrahydrofuran (THF)	24 h	500	80
Reflux	Acetone	24 h	500	76
Reflux	Ethanol	24 h	500	76
Reflux	Methanol	24 h	500	80
Reflux	Methanol	24 h	1000	90
Ultrasonication	Methanol	5 min	500	39
Ultrasonication	Methanol	30 min	500	45
Ultrasonication	Methanol	1 h	500	43
		$PrSO_3$-SBA-15		
Reflux	Toluene	24 h	500	62
Reflux	THF	24 h	500	69
Reflux	Acetone	24 h	500	78
Reflux	Ethanol	24 h	500	72
Reflux	Methanol	24 h	500	74
Reflux	Methanol	24 h	1000	89
Ultrasonication	Methanol	5 min	500	89
Ultrasonication	Methanol	5 min	100	90
Ultrasonication	Methanol	1 h	500	90

[a]Reflux method and ultrasonic extraction were conducted at 60 °C and room temperature, respectively.

inhabiting, the interaction between Fe(III) and cationic silicate species (I^+); As a result, employing Fe−H_2O_2 reagents, nonionic surfactant (S^0) was efficiently removed from SBA-15.

Although the microwave-assisted treatment has some advantages such as efficient and quick elimination of the organic template, less shrinkage of the framework, and less energy consumption, it suffers several drawbacks including difficulty in controlling the conditions of the microwave-assisted treatment in the case of some mesoporous materials, emission of CO_2 and toxic gases at the end of process due to the decomposition of surfactant, using solvents for assisting the process, and inability to recover or reuse the surfactant.[51,52]

2.1.4. Ultrasonic-Assisted Treatment. The ultrasonic technique is the well-defined process based on sonochemistry principles in which molecules undergo a chemical reaction owing to the application of powerful ultrasound irradiation (20 kHz−10 MHz).[53,54] Essentially, there is no chemical reaction during the direct interaction of ultrasonic radiation with the molecules; however, when ultrasonic radiation interacts with liquid, an alternating pattern of pressures is developed. Indeed, the acoustic cavitation (process of bubble formation, growth, and collapse under altering pressure) happens due to the interaction of ultrasonic radiation with the liquids and release of the accumulated ultrasonic energy in the bubbles producing energy with a very high local temperature of 5000 K and pressure of 1000 bar in few microseconds,[55−59] as shown in Figure 6(a).

Figure 6(b) depicts a schematic of ultrasonic-assisted treatment. This method has been utilized for template elimination from the pores of mesoporous materials. The ultrasonic treatment was used for detemplating MCM-41 by Jabariyan and Zanjanchi[60,61] for the first time and later by Pirez et al.[62] for template removal from SBA-15 and propylsulfonic acid ($PrSO_3H$)-functionalized SBA-15.

Jabariyan and Zanjanchi[60] have optimized the template removal conditions assisted by ethanol such as sonication time and temperature. The results disclosed that the S_{BET} and V_T values increased as the sonication time and temperature increased within the studied ranges. Longer sonication time resulted in a slight reduction of S_{BET} thanks to the slight destruction to the mesoporous structure of MCM-41. At the temperature of 60 °C and sonication time of 30 min, MCM-41 exhibited a higher S_{BET} of 1325 $m^2\ g^{-1}$ and V_T of 0.471 $cm^3\ g^{-1}$ than calcined MCM-41 possessing the S_{BET} and V_T of 1276 $m^2\ g^{-1}$ and 0.454 $cm^3\ g^{-1}$, respectively. This confirms the efficiency of this method for the template removal from as-synthesized MCM-41.

Ultrasonication was shown to be an effective technique for removing P123 from $PrSO_3H$-SBA-15 by Pirez et al.[62] However, in the case of virgin SBA-15, there was a great difference between the P123 percentage removed by ultrasonic irradiation and reflux extraction. As shown in Table 3, ultrasonication was ineffective in removing the template from the synthesized SBA-15 in methanol, while template removal of 90% was obtained reflux extraction. This may indicate that thermal activation is required to overcome hydrogen bonding interactions between the P123 template and isolated silanol groups, or ultrasonic irradiation could be conducted at moderate temperature for example 60 °C. As reported by Jabariyan and Zanjanchi,[60] the rate of template extraction from MCM-41 is relatively fast under ultrasonic irradiation in ethanol at a temperature of 60 °C rather than 25 °C providing a higher S_{BET} and V_T.

On the other hand, the template was efficiently removed from $PrSO_3H$-SBA-15 under ultrasonic irradiation in comparison to the solvent extraction method (as will be discussed later). As shown in Table 3, template extraction using methanol was more efficient than other studied solvents. After the second reflux with methanol, about 89% template was removed, as confirmed from Thermogravimetric analysis (TGA) between 150 and 350 °C. Using reflux for extraction of template required a long time about 24 h consuming 3600 W. Therefore, methanol was used for ultrasonic irradiation. The obtained result is interesting so that the template was

https://doi.org/10.1021/acs.energyfuels.1c04435
Energy Fuels XXXX, XXX, XXX−XXX

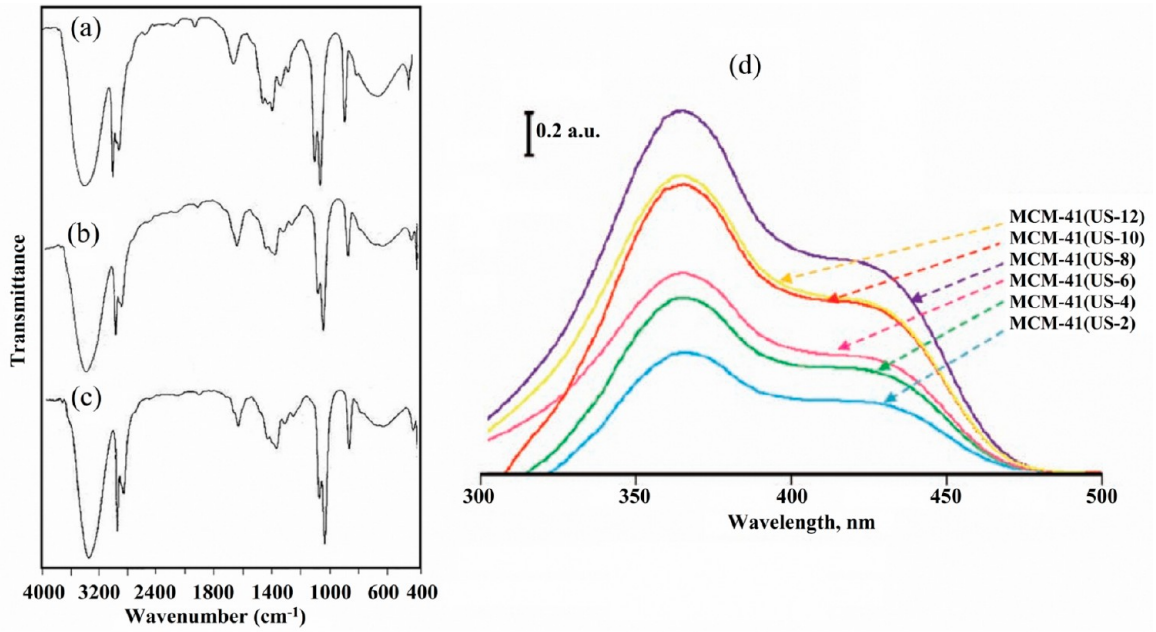

Figure 7. FT-IR spectra of (a) fresh CTABr-ethanol solution, (b) effluents after 15 min sonication at 40 °C, and (c) effluents after 60 min sonication at 40 °C. Panels (a) and (b) were reproduced from ref 60. [Jabariyan, S.; Zanjanchi, M. A. A simple and fast sonication procedure to remove surfactant templates from mesoporous MCM-41. *Ultrason. Sonochem.* **2012**, *19* (5), 1087−1093]. Copyright 2012 Elsevier. (d) UV−vis spectra for the methanol−effluent solutions after sonication at 40 °C and different times. Reproduced from ref 61. [Zanjanchi, M. A.; Jabariyan, S. Application of ultrasound and methanol for rapid removal of surfactant from MCM-41. *J. Serb. Chem. Soc.* **2014**, *79* (1), 25−38]. Copyright 2014, Serbian Chemical Society.

efficiently removed from the pores within 5 min at room temperature using ultrasonic irradiation consuming about 3 W. Their results disclosed that ultrasonic irradiation leads to a less lattice shrinkage of $PrSO_3H$-SBA-15 which possessed a higher a_0 of 11.2 nm and the pore wall thickness of 5.1 nm in comparison to that of $PrSO_3H$-SBA-15 treated by solvent extraction having a_0 of 11 nm and the pore wall thickness of 4.9 nm. All of these findings suggest that ultrasonic-assisted treatment is an efficient method and comparable with SC−CO_2 and microwave methods.

One of the notable advantages of ultrasonic-assisted treatment is that the recovery of the template is possible at the end of the template removal process. Jabariyan and Zanjanchi[60] studied the structure of the template removed from MCM-41 after sonication. Figure 7(a) displays the FT-IR spectrum of the CTABr−ethanol mixture for the sake of comparison. Figure 7(b) and (c) depicts FT-IR spectra of effluents obtained after 15 min sonication at 40 °C and 60 min sonication at 60 °C, respectively. As seen in Figure 7(a)−(c), the spectra of all samples were similar, indicating that the structure of CTABr was preserved after sonication in ethanol. In another study,[61] these authors investigated the concentration of CTABr after ultrasonic irradiation using a double-beam UV spectrophotometer. As shown in Figure 7(d), the concentration of CTABr was increased by increasing the sonication time; however, further increasing sonication time resulted in a decrease of CTABr concentration indicating that degradation of CTABr happened at longer sonication times. During ultrasonic irradiation, the surfactant molecules migrate apart from each other, causing micelle disruption in the alcohol solution. This matter was already well established in the field of drug delivery.[63−65] It was stated that ultrasonic vibrations cannot damage the hydrophobic tail of the organic template flocked in the micelle core. By acceleration of micelle disruption, they converted to monomers. The hydroxyl radicals ($HO^{\bullet}$) attack these monomers through the hydrophilic head of micelles in bulk solution; consequently, their nature is changed as a monomer in the CTABr structure. Therefore, provided that only micelle disruption happens during the ultrasonic irradiation, the structure of the surfactant removed by ultrasonic treatment is unaffected in alcohol and may be utilized for further synthesis.

2.1.5. Ozone Treatment. Low-pressure mercury lamps are applied in ozone generation. These lamps will emit ultraviolet (UV) light with two peaks in the UV light band, one at 254 nm with the energy of 472 kJ/mol and another at 185 nm with the energy of 647 kJ mol^{-1}. Since these energy values are higher than bonding energies in organic compounds such as C−H (413 kJ mol^{-1}), C−C (348 kJ/mol), and C−O (352 kJ mol^{-1}); UV lights are capable of removing the template at room temperature by breaking these bonds in the organic template.[66,67] The UV lamp is protected by a quartz tube, and both together are placed at the central axis of a reactor chamber. By passing air or O_2 through the chamber, it is subjected to photolysis of the O_2 molecule resulting in the formation of ozone.

Keene et al.[68] used this method for the first time to remove surfactant from MCM-41. In their study, ozone was generated from a simple UV lamp from atmospheric O_2 at room temperature (although the temperature within the pores of MCM-41was higher). The FT-IR and TGA results indicated that the template was efficiently removed from MCM-41. However, the reaction time was longer by about 24 h, and CO_2 is generated at the end of the process. Later, since the amount of generated ozone cannot be adjusted, and the reaction was long because of the low concentration of ozone (less than 1% by weight), instead of using a UV lamp, they employed an ozone generator.[69] To reduce the reaction time, ozone was

https://doi.org/10.1021/acs.energyfuels.1c04435
Energy Fuels XXXX, XXX, XXX−XXX

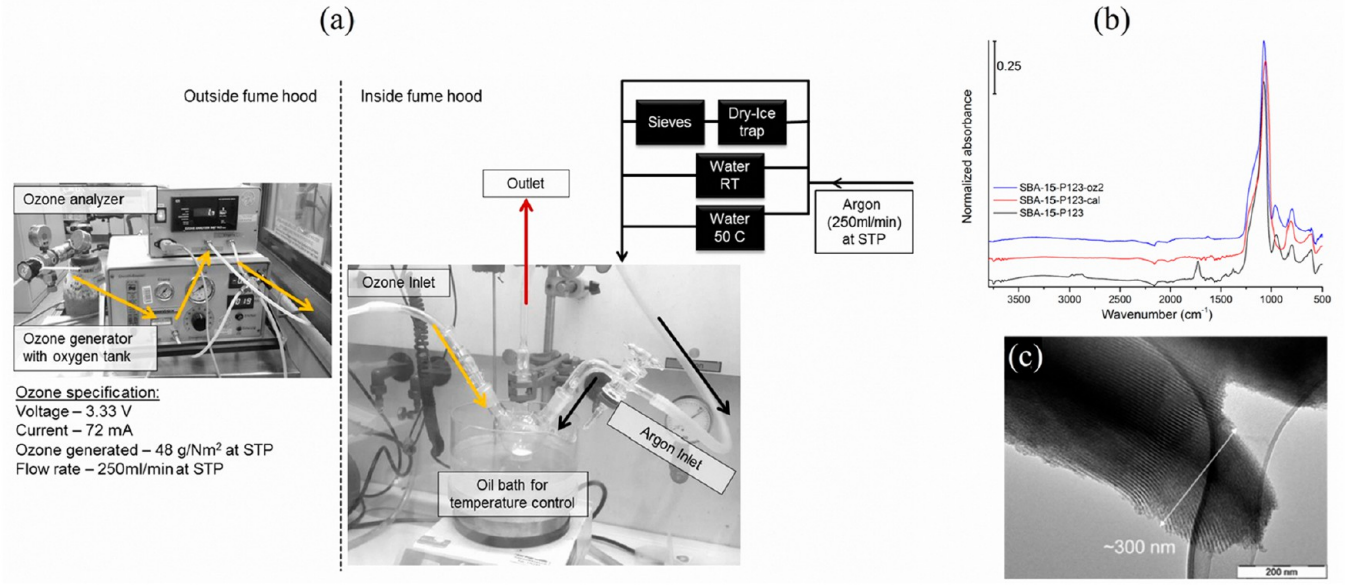

Figure 8. (a) Schematic of ozone treatment set up, (b) normalized ATR spectra of samples, and (c) TEM image of SBA-15 treated by H_2O_2. Reproduced from ref 70. [Joshi, H.; Jalalpoor, D.; Ochoa-Hernández, C.; Schmidt, W.; Schüth, F. Ozone Treatment: A Versatile Tool for the Postsynthesis Modification of Porous Silica-Based Materials. *Chem. Mater.* **2018**, *30* (24), 8905−8914]. Copyright 2018, American Chemical Society.

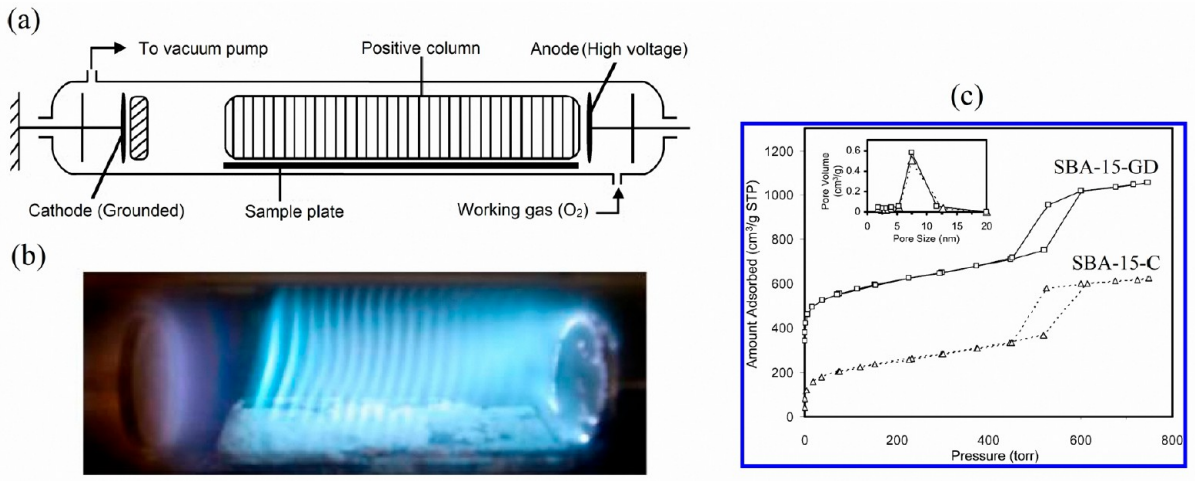

Figure 9. (a) Schematic of GD plasma, (b) loaded sample on a quartz boat placed in the positive column of O_2-forming GD, and (c) N_2 isotherms and BJH pore size distributions (inset) of SBA-15-C and SBA-15-GD. Reproduced from ref 78. [Yuan, M.-H.; Wang, L.; Yang, R. T. Glow Discharge Plasma-Assisted Template Removal of SBA-15 at Ambient Temperature for High Surface Area, High Silanol Density, and Enhanced CO_2 Adsorption Capacity. *Langmuir* **2014**, *30* (27), 8124−8130]. Copyright 2014, American Chemical Society.

generated via an electric discharge method. Their results showed that most of the CTABr surfactants were removed after 14 h from MCM-41 with a high S_{BET} of 1019 $m^2\ g^{-1}$ and pore diameter of 2.7 nm as well as a 5.52% carbon percentage. The structure of MCM-41 collapsed when the ozonation period was increased up to 26 h. Also, it was reported that template removal efficiency is lowered if the ozonation time is less than 14 h.[52,69]

Joshi et al.[70] used ozone treatment for P123 removal from as-synthesized SBA-15 at 80 °C for 120 min. Figure 8(a) shows the ozone reaction setup. It was stated that the carbon backbone of the P123 copolymer is highly oxygenated; thus, it reacts easily with ozone, causing the polymeric chains to become oligomers and further oxidation of the polymeric chains to occur through alcoholic and carbonyl groups. The results revealed that SBA-15 treated by ozone has a surface area of 711 $m^2\ g^{-1}$ which was comparable with that of calcined SBA-15 (749 $m^2\ g^{-1}$). Also, Barett−Joyner−Halenda (BJH) pore size and V_T values for SBA-15 treated by ozone were higher than calcined SBA-15. The remained carbon values for both SBA-15 treated by ozone and calcination were 3% and 0.5%, respectively. As shown in the IR spectroscopy spectra, the intensity of C−H vibration bonds decreased significantly after ozone treatment indicating the elimination of the P123 copolymer from SBA-15 (Figure 8(b)). Moreover, the transmission electron microscopy (TEM) image shows that SBA-15 treated by ozone is a highly ordered structure (Figure 8(c)). The template removal efficiency of ozone treatment through the TGA analysis was not investigated by Joshi et al.[70]

https://doi.org/10.1021/acs.energyfuels.1c04435
Energy Fuels XXXX, XXX, XXX−XXX

in order to compare with calcination or other methods discussed here.

The $OH^{\bullet}$ radicals can be generated by UV light in conjunction with H_2O_2 to get rid of organic contaminants in wastewater.[71,72] In this process, organic pollutants are oxidized to CO_2 and water by $OH^{\bullet}$ radicals produced by the interaction between ultraviolet light and H_2O_2. Later, Xiao et al.[73] used the UV/H_2O_2 process to eliminate the P123 copolymer from as-synthesized SBA-15 by dispersion in an aqueous solution of H_2O_2 and adjusting pH values with hydrochloric acid (HCl). Then, the mixture was irradiated using a medium-pressure Hg light for 3 to 4 h while stirring. The pH of the aqueous solution of H_2O_2 had a great influence on the physicochemical properties of the sample. The rate of formation of $OH^{\bullet}$ radicals and their reactions with organic molecules are affected by pH. TGA results showed that the template can be more completely removed at lower pH than higher pH. Moreover, the sample treated at higher pH had a lower S_{BET} and smaller V_T than the sample treated under acidic conditions. The main disadvantages of this method can be that the organic templates cannot be recovered, and toxic gases are produced leading to pollution of the environment.[35]

2.1.6. Plasma Technology. Nonthermal plasma (NTP) or cold plasma is an efficient method to eliminate organic molecules through a highly oxidizing environment at ambient temperature. The glow discharge (GD) and dielectric barrier discharge (DBD, or silent discharge) are two examples of NTP which have been used to degrade templates from zeolite and mesoporous silica materials.[74−80]

For the production and treatment of catalysts, GD is employed as NTP with a high electron temperature (10^4−10^5 K) and a low gas temperature (as low as room temperature) because it is energy efficien and works at very mild conditions, and its operational time is shortened.[81−84] A schematic of GD plasma is depicted in Figure 9(a). It comprises two electrodes in a chamber that is filled with O_2 as the plasma-forming gas after evacuation to below 1 Torr. The temperature of GD plasma could be lower than 50 °C. To prevent the entering of fine particles into the vacuum pump, a few drops of water are added to the SBA-15 before starting the template removal. Figure 9(b) shows the moving striations observed in the positive column when the as-synthesized SBA-15 is loaded. Then, in this positive column, the template is decomposed due to a strong interaction between the fluxes of plasma-active species (e.g., O^{2+}, O, electron) and the SBA-15 surface. The color of the glow is determined by the type of gas in the tube. A blue-violet color is observed in the glow discharge plasma shown in Figure 9(b) because the chamber was fed with O_2 as the plasma-forming gas. It should be noted that some gases are produced during template removal which could influence the GD performance; therefore, the amount of O_2-forming GD gas should be sufficient for maintaining the stable discharge plasmas. The elemental analysis result shows that the carbon contents of the SBA-15 template were removed by GD plasma (SBA-15-GD) over 120 min and calcination (SBA-15-C) at 550 °C for 5 h under the heating rate of 1.75 °C min^{-1} were 1.28% and 0.3%. These results indicate that the template removal efficiency of GD plasma is much higher than that of methanol extraction, as discussed before. Figure 9(c) illustrates the N_2 adsorption−desorption isotherms of samples. From the obtained results, SBA-15-GD possessed a higher S_{BET} of 1025 m^2 g^{-1} than SBA-15-C with the S_{BET} of 827 m^2 g^{-1}. Moreover, the higher unit-cell size and the pore wall thickness of SBA-15-GD indicate that the shrinkage by GD is less than that by calcination because of applying low temperature for the elimination of the template. Also, it was found that more silanol densities are preserved on the surfaces by employing GD plasma rather than conventional calcination which is beneficial for postsynthesizing of silica support. Overall, it can be concluded that although about 94.8% of the template was removed by using GD plasma, the exposure time still is long at about 120 min.

DBD is generally considered a low-temperature plasma oxidation technology due to its operation under ambient conditions (at room temperature and atmosphere). DBD has been extensively utilized in many applications such as catalyst preparation and modification,[85−87] surface modification of nanofibers,[88] pollutant control (wastewater purification and engine exhaust control),[89−93] ozone generation,[94,95] hydrogen production from the reforming of biogas,[96] oxygen reduction reaction of electrocatalysts,[97] removal of volatile organic compounds (VOCs),[98,99] and remediation of pyrene and ciprofloxacin contaminated soil.[100−102] Recently, DBD was employed to eliminate the template from mesoporous materials,[75−77] particularly SBA-15.[74,80] The DBD plasma technology can be categorized into single dielectric-barrier discharge (SDBD) and double dielectric-barrier discharge (DDBD).

SDBD plasma is a promising technique that has exhibited a better performance to remove the template accompanied by less structure shrinkage and increased silanol density. A schematic of SDBD is shown in Figure 10(a) which has been employed for the template removal from SBA-15,[80] MCM-41,[76] and Zeolite Socony Mobil-5 (ZSM-5).[77] Wang et al.[80] used the SDBD reactor to eliminate the P123 copolymer from SBA-15. The FT-IR spectra of as-synthesis SBA-15, SBA-15-C, and SBA-15-DBD are illustrated in Figure 10(b). Normally, the aliphatic stretching and bending vibrations are observed at wavenumbers between 2950 and 2840 cm^{-1} and 1500−1350 cm^{-1}, respectively.[103] As can be seen in Figure 10(b), these peaks appeared in the spectrum of as-synthesized SBA-15 signifying the presence of P123 copolymer. However, it was completely removed after SDBD treatment and calcination. Another interesting feature of Figure 10(b) is that there was a dramatic decrease in the intensity of the Si−OH bending band after calcination thanks to the dehydroxylation at higher temperatures for a prolonged time. The intensity of the Si−OH bending band of SBA-15-DBD is almost the same as the as-synthesized SBA-15, indicating that the DBD treatment can preserve more silanol groups on the pore wall as already proved from template removal of SBA-15 via GD plasma. The remaining silanol groups were further confirmed by ^{29}Si solid sate NMR spectra. Figure 10(c) shows the N_2 sorption−desorption isotherms of SBA-15-C and SBA-15-DBD together with their physicochemical properties. The wall thicknesses of both samples are the same, while SBA-15-DBD possessed higher S_{BET}, V_T, and larger pore size values because of the less lattice shrinkage in comparison to SBA-15-C treated at high temperature.

Aumond et al.[74] used a quartz reactor for template removal of SBA-15. A mixture of 80/20 helium/O_2 was used as the feed gas. It has been well established that helium is a better energy carrier, and using this gas can considerably reduce plasma treatment time. The results showed that the pronounced lattice shrinkage by NTP is less because of the development of ultramicroporosity and larger hexagonal structured mesoporos-

https://doi.org/10.1021/acs.energyfuels.1c04435
Energy Fuels XXXX, XXX, XXX−XXX

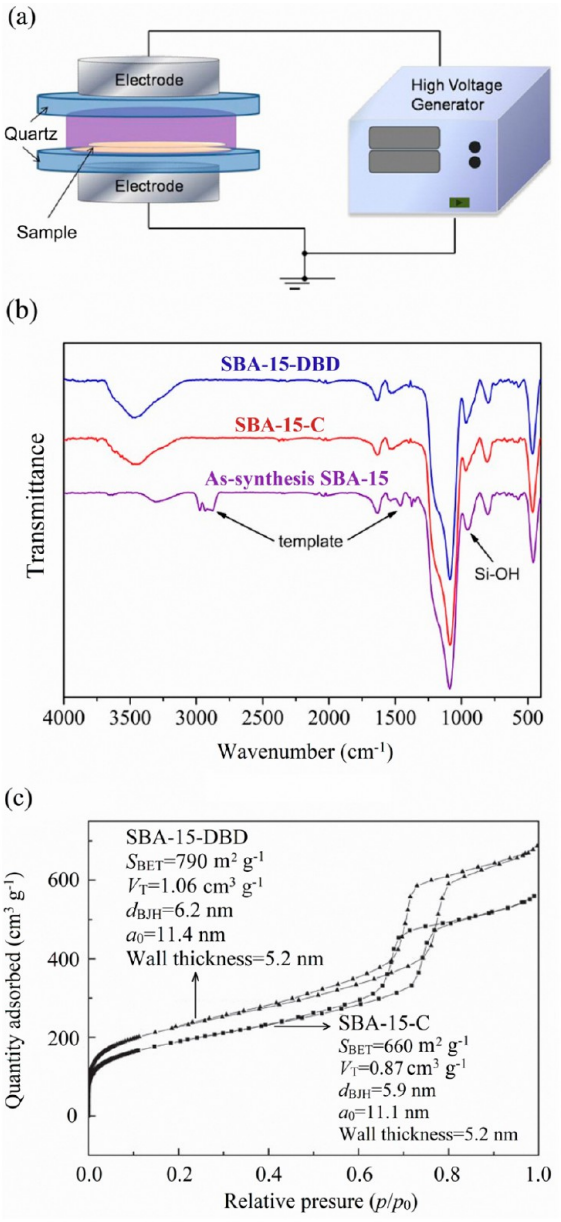

Figure 10. (a) Schematic of the SDBD apparatus. Reproduced from ref 85. [Guo, Q.; With, P.; Liu, Y.; Gläser, R.; Liu, C.-j. Carbon template removal by dielectric-barrier discharge plasma for the preparation of zirconia. *Catal. Today* **2013**, 211, 156−161]. Copyright 2013, Elsevier. (b) FT-IR spectra of samples and (c) N_2 sorption−desorption isotherms of the sample treated by calcination and NTP along with their physicochemical properties. Panels (b) and (c) were reproduced from ref 80. [Wang, L.; Yao, J.; Wang, Z.; Jiao, H.; Qi, J.; Yong, X.; Liu, D. Fast and low-temperature elimination of organic templates from SBA-15 using dielectric barrier discharge plasma. *Plasma Science and Technology* **2018**, 20 (10), 101001]. Copyright 2018, IOPscience.

ity in comparison with the calcination method. Since NTP using a quartz reactor is working at room temperature, more silanol densities were preserved on the surfaces. Another advantage of using this method is that a less exposure time of about 15 min is needed for the template removal. The authors did not explain further the reaction mechanism of the template degradation using NTP. The interaction between the SBA-15 powder surface and active species such as positive ion O^{2+} and negative ions O^- and O^{2-} as well as O^3 resulted in the decomposition of the template. Indeed, the composition of the exhaust gases (mainly CO and CO_2 associated with H_2O) indicated direct oxidation of the template molecules.

Alternatively, plasma in an aqueous solution, also known as solution plasma, is a high potential plasma that was used to remove templates. Pootawang et al.[104,105] used the solution plasma process to eliminate the P123 template from mesoporous silica materials, as depicted in Figure 11(A). Various active species, such as high active radicals (e.g., $H^•$, $O^•$, $OH^•$, $HO_2^•$), high energy electrons, and UV radiation can be physically created during discharge in an aqueous solution. The effects of discharge solution pH and discharge time were investigated on the template removal. There is no substantial variation in the intensity of the first peak in the small-angle X-ray diffraction (SAXRD) patterns shown in Figure 11(B), but the strength of the second peak was clearly identified in the different amounts.

The intensity of the second peak was lower at a pH of 7, while the sample exhibited a high intensity of the second peak when the pH of the discharge solution was adjusted to 7 or 11. This result indicates a high capability of the template removal process in acid and base solutions rather than neutral pH. Figure 11(C) shows the effect of discharge time on structural properties. As seen in Figure 11(C), the second peak intensity was much higher at the discharge time of 15 min. This result demonstrated that the rate of organic decomposition increased as discharge duration increased and was influenced by the number of active species, which had a strong tendency to create more as the system's temperature and energy increased. The parallel channels with a uniaxial cylindrical mesopore arrangement are visible in the TEM images presented in Figure 11(D)−(F). The structural morphology of the mesopore structure was unaffected by changes in pH and discharge time.

Despite its advantages, for instance, simple experimental setup, stable and reproducible plasma conditions, and operating at atmospheric pressure and relatively low temperature,[78,85,99] SDBD plasma still has some significant limitations, including the need for a greater electrical voltage to create a strong electric field and the deposition of solid byproducts on the reactor's inner surface and electrodes, which affect its performance. DDBD plasma technology is a modified version of SDBD plasma that has a better discharge efficiency and longer electrode lifespan.[49] DDBD plasma has been mostly utilized to remove air pollutants, particularly VOCs.[98,99] So far, there is no report on using DDBD plasma for template removal; therefore, DDBD plasma can be utilized for the template elimination from mesoporous siliceous materials. Furthermore, the plasma solution technique has some drawbacks, including the need for a high voltage to generate a continuous plasma discharge and low energy efficiency.

The oxidation mechanism of template elimination for the production of molecular sieves such as MCM-41 and ZSM-5 using DBD plasma was studied by Liu et al.[75] As illustrated in Figure 12(a), the infrared image showed that the template was removed at the highest temperature of 125 °C for 75 min. As can be seen in Figure 12(c), the color of MCM-41 was changed during template removal by increasing time. The fresh white sample became yellow after 15 min, showing that the template and plasma species were reacting. By increasing the time to 60 min, the sample became brown. The sample becomes white again after around 75 min. This marks the end of the template removal process. The mechanism study of

https://doi.org/10.1021/acs.energyfuels.1c04435
Energy Fuels XXXX, XXX, XXX−XXX

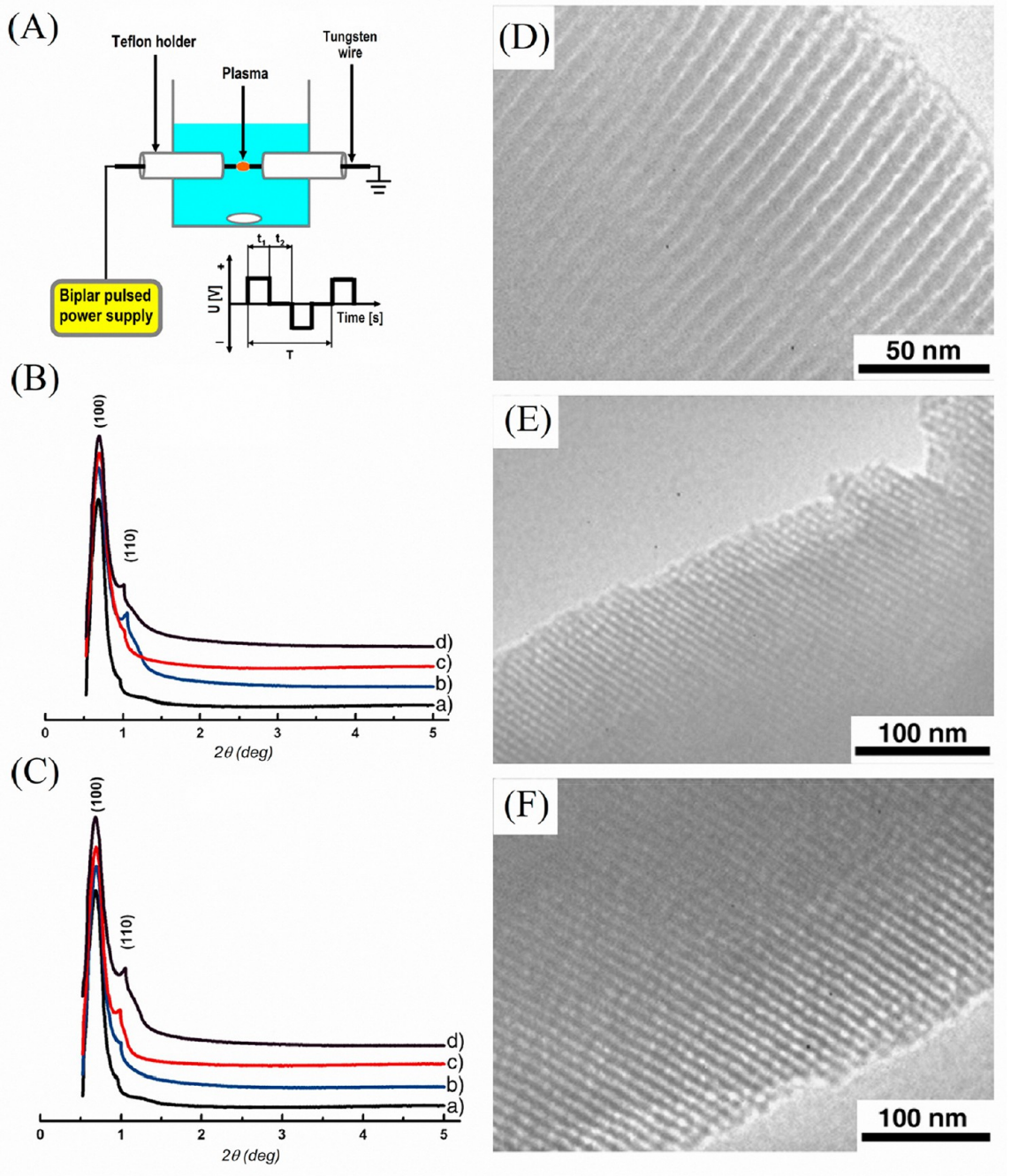

Figure 11. Plasma solution process. (A) Scheme image of the solution plasma experimental setup. (B) SAXRD patterns of mesoporous silica discharged in different pHs at fixed 15 min of discharge time: (a) as-synthesized silica, (b) pH 3, (c) pH 7, and (d) pH 11. (C) SAXRD patterns of mesoporous silica discharged at different discharge times in pH 3: (a) as-synthesized silica, (b) 1 min, (c) 5 min, and (d) 15 min. TEM images of mesoporous silica discharged in different pH values at fixed 15 min of discharge time: (D) pH 3, (E) pH 7, and (F) pH 11. Reproduced from ref 104. [Pootawang, P.; Saito, N.; Takai, O. Solution plasma for template removal in mesoporous silica: pH and discharge time varying characteristics. *Thin Solid Films* **2011**, 519 (20), 7030−7035]. Copyright 2015, Elsevier.

template removal under DBD plasma is difficult due to complex reactions between active species and template molecules. The electrons play a vital role in the dissociation of template molecules. The energetic electron bombardment can decompose template molecules producing H_2 and methane gases during the process. CO_2 is also formed through oxidation with active oxygen species (O and O_3). During the template elimination from MCM-41, mass spectra of gases revealed the presence of N_2O gas as one of the products. As shown in Figure 12(b), FT-IR results of MCM-41 confirmed that MCM-41 templates are removed using DBD plasma so that C−H stretching and bending vibrations disappeared completely after 75 min. Also, the oxidation of nitrogen species in the organic template was observed by bands appearing at a wavenumber of about 1384 cm^{-1} from 15 to 60 min.

2.2. Chemical Methods. *2.2.1. Solvent Extraction.* Template extraction using solvents is a common method for template removal,[106−121] as shown in Figure 13. de Ávila et al.[107] used different solvents such as water, acetonitrile, dichloromethane, ethanol, acetone, and methanol to eliminate

https://doi.org/10.1021/acs.energyfuels.1c04435
Energy Fuels XXXX, XXX, XXX−XXX

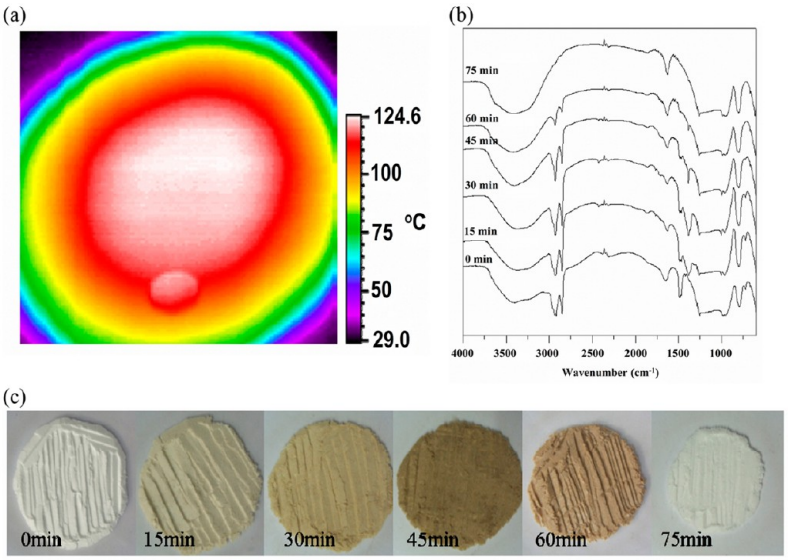

Figure 12. (a) Infrared image of the sample during the template removal process using DBD. Reproduced from ref 77. [Liu, Y.; Pan, Y.-x.; Kuai, P.; Liu, C.-j. Template Removal from ZSM-5 Zeolite Using Dielectric-Barrier Discharge Plasma. *Catal. Lett.* **2010**, 135 (3), 241−245]. Copyright 2010, Springer. (b) FT-IR spectra of MCM-41 during the detemplating process using DBD plasma. (c) Color changes of the samples during the template removal using DBD. Panels (b) and (c) were reproduced from ref 75. [Liu, Y.; Wang, Z.; Liu, C.-j. Mechanism of template removal for the synthesis of molecular sieves using dielectric barrier discharge. *Catal. Today* **2015**, 256, 137−141]. Copyright 2015, Elsevier.

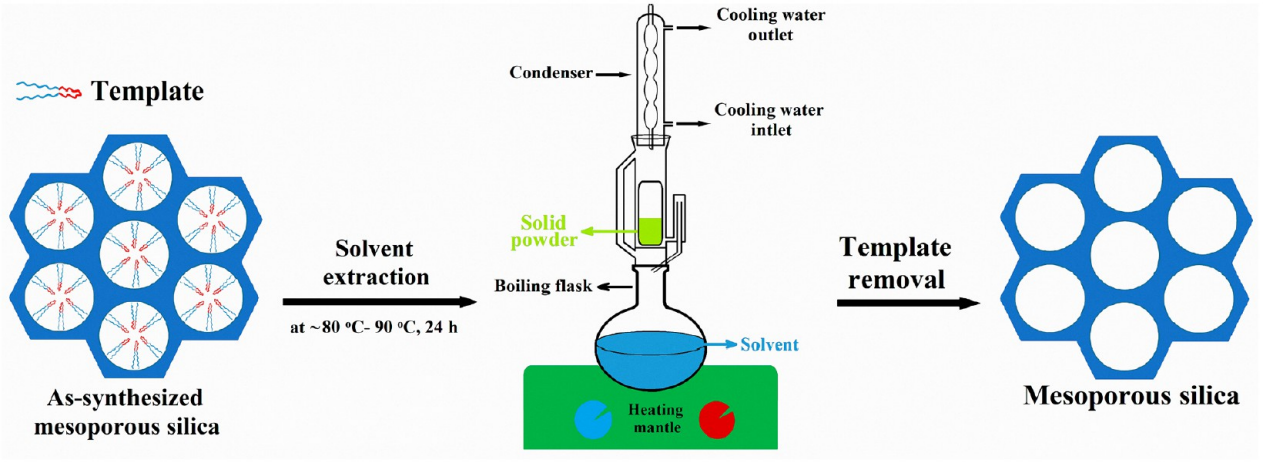

Figure 13. Schematic of solvent extraction technique.

the template from SBA-15 pores. The results indicated that water had the lowest effect on the template extraction, and the amount of remained P123 template was about 45.9% which was almost the same as the not-extracted one. Among studied solvents, however, methanol has the highest efficiency to remove the template. After template extraction using methanol, SBA-15 possessed about 10.3% of P123, and the result was in agreement with the amount of C of about 4.8% obtained from elemental analysis. The S_{BET}, V_T, and pore diameter of SBA-15 extracted with methanol were 703 $m^2\ g^{-1}$, 0.995 $cm^3\ g^{-1}$, and 15.2 nm, respectively. Moreover, the effect of extraction time on template removal was investigated using the aforementioned solvents. The results indicated that less extraction time of about 6 h is enough to remove the template when methanol was used as the extraction solvent in comparison to other solvents with a longer extraction time of up to 48 h to complete the template extraction. Chun et al.[122] used several solvents for extraction of pluronic F-127 such as methanol, ethanol, acetone, *n*-hexane, and iso-propanol. It was found that when methanol was employed as the solvent extraction, the highest efficiency of 78.8% was obtained. The above-mentioned results indicate that methanol has a better performance to remove the templates among polar and nonpolar solvents. A mixture of HCl and ethanol was reported for extractions of P123 and CTABr from SBA-15[123,124] and MCM-48,[125] respectively. Sulfuric acid (H_2SO_4) was used to extract F-127 and P123 from a mesostructured polymer−silica composite[126] and SBA-15,[124] respectively, and also a mixture of H_2SO_4 and sodium hydroxide (NaOH) was utilized for removal of a P123 copolymer from SBA-15.[124] To generate mesopores and micropores in SBA-15, Schüth et al.[127] used H_2SO_4 under reflux at 95 °C for 24 h to partially remove a P123 copolymer from as-synthesized SBA-15 followed by calcination to decompose the occluded poly(ethylene oxide) chains in the silica matrix and to create micropores. The authors demonstrated that the ether cleavage by sulfuric acid at

https://doi.org/10.1021/acs.energyfuels.1c04435
Energy Fuels XXXX, XXX, XXX−XXX

quite a low temperature resulted in the formation of mesopores due to the elimination of the PO groups. Following a thermal treatment in air at 200 °C to produce micropores, the EO chains, which are less accessible to the acid, may be destroyed. Thus, SBA-15 material with superior properties than the traditional calcined SBA-15 material has resulted from such acid and low-temperature treatments (larger mesopore size, larger micropore volume). However, this process is time consuming and requires two stages to remove the template from as-synthesized SBA-15.

Grudzien et al.[128] used a combination of solvent extraction (ethanol/HCl) and temperature-controlled calcination to remove F-127 from SBA-16. Their results showed that SBA-16 has a higher S_{BET}, V_T and pore diameter and less framework shrinkage when the template was removed using this combination method in comparison to calcination alone, although the carbon percentage of the latter one was less than the former one. A mixture of ethanol/HCl with a molar ratio of (1:1) was used to remove mixed anionic surfactants such as sodium dodecyl benzenesulfonate (SDBS) and sodium dodecyl sulfate (SDS) from mesoporous silica materials.[129] The pore size distribution showed two narrow and broad peaks located at 10.3 and 30.7 nm, respectively. Samples had a low S_{BET} of 217 m^2 g^{-1}. The formation of large pores indicates that a mixed anionic surfactant could be removed from the pores during solvent extraction. The mixture of ethanol−HCl was also used to remove CTAB from SBA-1 synthesized by cocondensation of TEOS and phenyltriethoxysilane (PhTES).[114] When the TEOS/PhTES molar ratio was (7:1), SBA-1 exhibited S_{BET} and V_T of 980 m^2 g^{-1} and 0.47 cm^3 g^{-1}, respectively. The S_{BET} and V_T values were reduced when this ratio was reduced. The TGA data, on the other hand, revealed that surfactant remained in the pores of SBA-1, particularly at lower TEOS/PhTES molar ratios. The same result was reported for mesoporous silica material grafted by aminopropyltriethoxysilane (APS).[130]

Another study showed the removal of SDS using the mixture of HCl and acetonitrile so that 89% of SDS was removed as conformed by elemental analysis.[131] Yokoi et al.[132] used the mixture of HCl and acetonitrile to remove the SDBS, SDS, and lauric acid sodium salt (LAS) anionic surfactants from pores. The elemental analysis results showed that 88%, 89%, and 91% of SDBS, SDS, and LAS surfactants were removed, respectively, following the solvent extraction at room temperature for 2 h. The final powder was unstable when SDBS was used as a surfactant upon the solvent extraction. Also, the extracted samples had a lower S_{BET} than calcined counterparts due to the retention of aminopropyl moieties on the surface.

Rahman et al.[133] used 5 wt % aqueous dimethyl sulfoxide (DMSO) solution to remove the template from mesoporous silica synthesized using sodium silicate as a silica source from bagasse ash. The sample extracted by a 5 wt % aqueous DMSO solution showed a typical type IV isotherm with an H2 type of hysteresis indicating the mesoporosity of the obtained material. The extracted sample exhibited a higher S_{BET} of 656 m^2 g^{-1} than the calcined sample, which had an S_{BET} of 486 m^2 g^{-1} at pH 3. The process of template removal has a substantial impact on the pore volume. The pore volume of silica obtained during solvent extraction was approximately 0.8 cm^3 g^{-1}, while that obtained through calcination was around 0.2 cm^3 g^{-1}. For solvent extraction, the pore diameter increases dramatically as the pH rises, but it remains relatively constant for calcination. The pore diameter was around 4 nm for calcination, and it varies from 3 nm at pH 2 to 18 nm at pH 7 for solvent extraction.

Solvent extraction was employed to remove dual templates of F-127 and P123 from SBA-16 functionalized by carboxyethylsilanetriol sodium salt (CES) using 8 wt % H_2SO_4 solutions.[118] After solvent extraction, the sample had S_{BET} and V_T of 575 m^2 g^{-1} and 0.71 cm^3 g^{-1}, respectively, and exhibited a sharp diffraction peak with a higher intensity in comparison to as-synthesized counterpart. Also, after acid extraction, the TEM image demonstrated the presence of distinctive pores of ordered mesoporous silica. Although these findings show that acid extortion is a viable strategy for removing the template from surface-functionalized mesoporous silica materials, template removal takes a longer duration of 24 h.[118]

Zhou et al.[134] used solvent extraction with acetonitrile in an autoclave at 90 °C to remove IL as a template from mesoporous silica, namely, 1-butyl-3-methyl-imidazolium-tetrafluoroborate, $[C_4mim]BF_4$. The FT-IR revealed that imidazolium $\nu_{(C-H)}$ stretching region (3200−3000 cm^{-1}) of the IL vanishes completely. The sample had S_{BET} and V_T of 801 m^2 g^{-1} and 1.27 cm^3 g^{-1}, respectively. These results indicate the effectiveness of solvent extraction in IL removal from the pores. Although IL was removed completely, the extraction was repeated several times, and a high volume of solvent was used.

The solvent extraction method is more advantageous than the calcination method because more silanol groups can be preserved, and shrinkage of pores is not significant after template extraction. However, the solvent extraction method is far from practical application. From the economic and environmental perspectives, this method is not beneficial due to a large volume consumption of organic solvent and the required high energy for solvent recovery. Above all, the template may not be completely removed even when the extraction treatment is repeated several times.

2.2.2. Chemical Oxidation. H_2O_2 treatment is based on an advanced oxidation process where the surfactant decomposition happens by in situ $HO^\bullet$ generation. The Fenton-based oxidation process is frequently applied for $HO^\bullet$ generation taking place in the presence of H_2O_2 and some metal ions (such as Ni, Fe, Bi, Cr, and Zn). H_2O_2 treatment catalyzed by Fe was applied to remove the template of MCM-41[135] and zeolite beta.[136,137] Later, Zhang et al.[138] used H_2O_2 for the generation of $HO^\bullet$ catalyzed by Fe cations to eliminate the template of SBA-15 at 70 °C for 7 h. The following reactions show the template removal using H_2O_2 catalyzed by Fe^{3+} and Fe^{2+} cations. In reaction 5, $HO^\bullet$ radicals oxidize the organic template entrapped within the structure; finally, mesoporous material is obtained, and H_2O and CO_2 are generated (reaction 5).

$$H_2O_2 + Fe^{3+} \rightarrow HO_2^\bullet + H^+ + Fe^{2+} \quad (1)$$

$$H_2O_2 + Fe^{2+} \rightarrow OH^\bullet + OH^- + Fe^{3+} \quad (2)$$

$$OH^\bullet + Fe^{2+} \rightarrow OH^- + Fe^{3+} \quad (3)$$

$$OH^\bullet + H_2O_2 \rightarrow HO_2^\bullet + H_2O \quad (4)$$

$$SiO_x(OH)_{2-x}(\text{Surfactant}) + OH^\bullet \rightarrow SiO_x(OH)_{2-x}() + CO_2 + H_2O \quad (5)$$

https://doi.org/10.1021/acs.energyfuels.1c04435
Energy Fuels XXXX, XXX, XXX−XXX

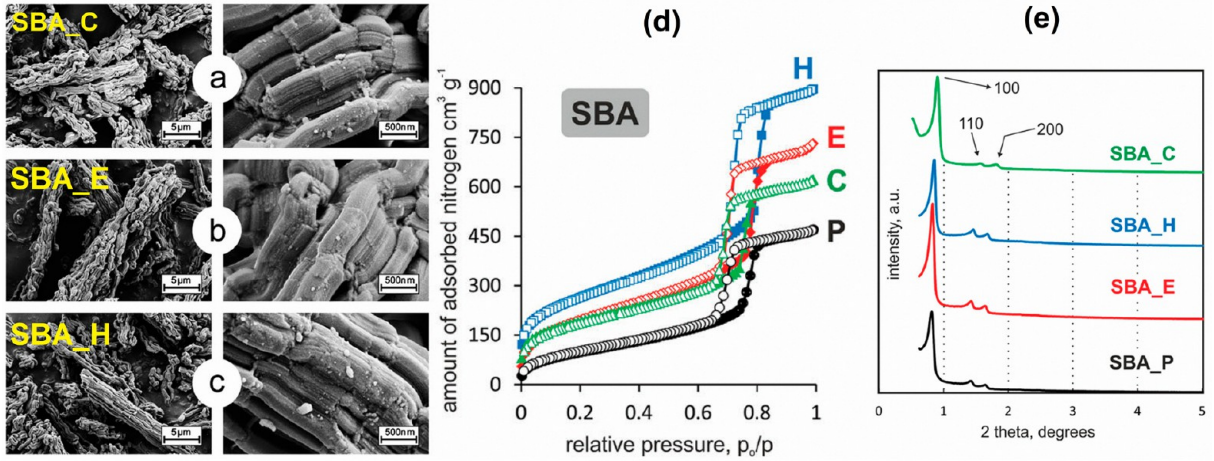

Figure 14. Characterization of SBA-15 materials treated by different methods: SBA_P, as-synthesized SBA-15; SBA_C, SBA-15 treated by calcination; SBA_E, SBA-15 treated by extraction; and SBA_H, SBA-15 treated by H_2O_2. (a)−(c) SEM images. (d) N_2 adsorption−desorption isotherms. (e) SAXRD patterns. Reproduced from ref 108. [Barczak, M. Template removal from mesoporous silicas using different methods as a tool for adjusting their properties. *New J. Chem.* **2018**, 42 (6), 4182−4191]. Copyright 2018, Royal Society of Chemistry.

The results showed that the carbon content of materials was significantly reduced to 0.4% and even more reduction to 0.2% when the template of SBA-15 was extracted by ethanol and then H_2O_2 treatment catalyzed by Fe cations. However, the carbon content of calcined SBA-15 was 0.1%. The SBA-15 treated by H_2O_2 had a higher silanol value of 44% than that of the calcined counterpart with a 30% silanol value determined by ^{29}Si NMR. Also, template removal using H_2O_2 increased S_{BET} and V_T of SBA-15 compared to conventional calcination.[138] Zhang and Melián-Cabrera[139] reported similar results. In their study, the effects of secondary treatments such as direct drying, hydrothermal treatment, and solvent exchange were investigated on the structural and textural properties of SBA-15.

On the other hand, this process has two main disadvantages of a long time for template removal and the limitation of mesoporous silica for desired application because of the existence of metal ions in the silica framework. Also, CO_2 is generated after completing the process, as mentioned above. It was reported that H_2O_2 has enough power to eliminate the template for pores of MCM-41 in the presence or absence of metal ions (Fe^{3+}) with a significantly shorter reaction time (1 h).[140] Later, Barczak[108] used the H_2O_2 treatment method without a Fenton reaction to remove the P123 copolymer from pores of SBA-15 at 108 °C for 3 h, and the results were compared with extraction and calcination methods. The carbon content of SBA-15 treated by H_2O_2 was 0.6% which is comparable with the results stated by Zhang et al.[138] with the Fenton reaction. Figure 14(a) displays the scanning electron microscope (SEM) images of SBA-15 treated by different methods. As can be seen, the SBA-15 materials had the same morphology of parallel hexagonal cylinders with a "sausage-like" shape. As displayed in Figure 14(b), the N_2 adsorption−desorption isotherms of SBA-15 materials showed a type IV isotherm according to the IUPAC classification associated with their mesoporous structure with hysteresis loops. Also, the results showed that SBA-15 treated by H_2O_2 exhibited a higher S_{BET} of 953 than those treated by extraction (688 m^2 g^{-1}) and calcination (726 m^2 g^{-1}). Moreover, from SAXRD patterns shown in Figure 14(c), it was found that the framework shrinkage is significantly reduced through H_2O_2 treatment and extraction; however, the first sharp reflection and the other two weak reflections were less intense and shifted toward higher values indicating the occurrence of framework shrinkage during calcination. As seen in Figure 14(c), two minor reflections were resolved well, and their intensities were higher for SBA-15 treated by H_2O_2 than that treated by calcination indicating a better organization obtained by surfactant removal via H_2O_2 treatment. Therefore, these results confirm that H_2O_2 treatment is an effective method to eliminate the most anchored poly(oxypropylene) blocks remaining with only very small amounts of the template in the pores. In another interesting effort done by Yang et al.,[141] the template was removed using H_2O_2 in the crystallization process. The coupling of the crystallization process and hydrothermal oxidation with H_2O_2 facilitates further condensation and slight framework shrinkage. The hydrothermal stability of materials was investigated using boiling water for 72 h under reflux. Their results showed that the sample treated by H_2O_2 could maintain about 86% of its specific surface, while the sample without H_2O_2 treatment had a less ordered structure and preserved only 24% of its specific surface area.

Lu et al.[142] used a chemical oxidation method at a low temperature of 60 or 90 °C with a duration of 4 or 24 h for template removal from SBA-15 using a potassium permanganate ($KMnO_4$)−H_2SO_4 solution as an oxidizer. This method was efficient for the purification of carbon nanotubes from amorphous carbons.[143] According to the findings, the temperature and reaction time have great effects on the formation of manganese oxide on the exterior surface of SBA-15. The reaction between the template and $KMnO_4$ is mainly controlled by temperature so that there is manganese oxide on the exterior surface at low temperature, while there is no deposition of manganese oxide on SBA-15 at higher temperatures (60 or 90 °C). Regarding the effect of reaction time, if the temperature is low, for example, room temperature, the reaction time should be longer. The SBA-15 treated by chemical oxidation at 90 °C for 24 h had a higher S_{BET}, V_T, and pore diameter of 940 m^2 g^{-1}, 1.42 cm^3 g^{-1}, and 9.8 nm, respectively, indicating better textual properties in comparison to calcined SBA-15. Compared with calcined SBA-15 with a_0 of 10.5 nm, the SBA-15 treated by $KMnO_4$ had a_0 = 11.8 nm,

https://doi.org/10.1021/acs.energyfuels.1c04435
Energy Fuels XXXX, XXX, XXX−XXX

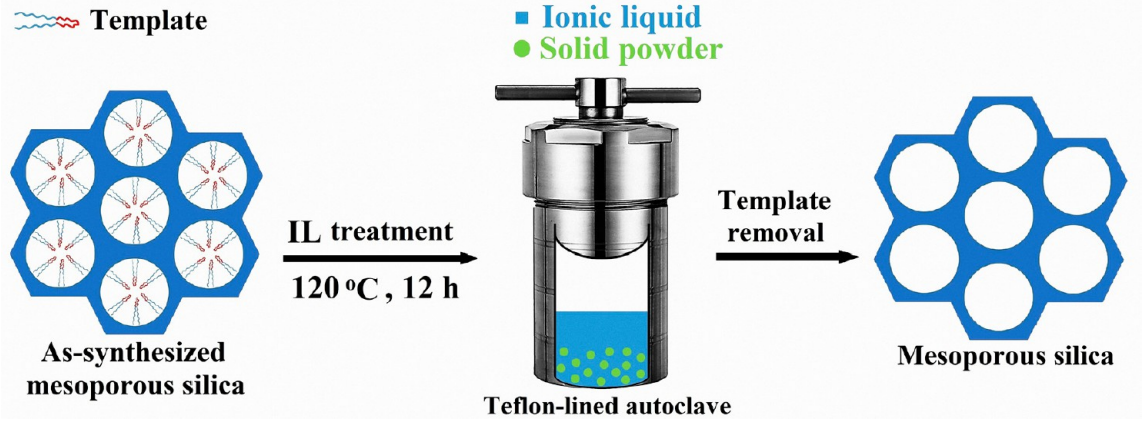

Figure 15. Schematic of IL treatment technique.

indicating less of a shrinkage structure during $KMnO_4$ treatment compared to calcination. Ding et al.[144] used HNO_3 oxidation to remove the P123 copolymer from SBA-15 at 100 °C for 12 h. Through this method, block copolymer P123 is easily oxidized into small molecules, such as formaldehyde, formic acid, acetaldehyde, acetic acid, and CO_2. The S_{BET}, V_T, and BJH pore size values for SBA-15 treated by HNO_3 oxidation were 714.6 $m^2\ g^{-1}$, 1.30 $cm^3\ g^{-1}$, and 6.79 nm, respectively, while those for calcined SBA-15 were 723.8 $m^2\ g^{-1}$, 0.86 $cm^3\ g^{-1}$, and 5.36 nm, respectively. Moreover, the positions of the diffraction peaks of the SBA-15 treated by HNO_3 oxidation were basically the same as those of as-synthesized SBA-15, while the positions of the diffraction peaks of calcined SBA-15 are obviously shifted to a high angle. This indicates less shrinkage of framework during HNO_3 oxidation treatment compared to calcination. The result showed that the removing ratio of the template of SBA-15 is 82.5%. The advantage of HNO_3 oxidation treatment over $KMnO_4$–H_2SO_4 solution treatment is that the reduction product can be easily removed by washing, therefore, avoiding the use of $KMnO_4$ or other metal oxidants in the process of oxidizing the template.

2.2.3. Ionic Liquid (IL) Treatment. The IL treatment is the last method used for template removal, as shown in Figure 15. The idea of using IL for template removal comes from biomass delignification. To increase the accessibility of enzymes to cellulose and in turn improve the hydrolysis process, removal of lignin as an organic polymer is necessary. Wang and Yang[145] used IL 1-butyl-3-methylimidazolium chloride ($[C_4mim]Cl$) to eliminate the P123 template from as-synthesized SBA-15 at 120 °C for 12 h and compared the results with conventional calcination at 500 °C for 6 h. The results revealed that the SBA-15 treated by calcination and IL showed BJH pore size distributions of 6.4 and 7.5 nm, respectively. This indicates that using IL treatment resulted in less shrinkage of the mesoporous framework structure compared to calcination. The TGA results showed that the P123 template was removed at least 92%, demonstrating that treatment was effective. Moreover, more silanol groups were retained in the SBA-15 framework treated by IL in comparison to that treated by calcination so that silanol numbers of SBA-15 treated by IL and calcination were 5.1 and 3.0 OH nm^{-2}, respectively. Moreover, SBET and V_T of SBA-15 treated by IL were 835.5 $m^2\ g^{-1}$ and 1.09 $cm^3\ g^{-1}$, respectively, which were comparable with the calcined counterpart. The template removal mechanism through IL treatment is similar to that of cellulose dissolution in ILs. The hydrogen bonds between the template P123 and the silanol groups on the surface are likely disrupted and broken by using IL so that the treated SBA-15 has a higher surface hydroxyl group density. The template removal at the low temperature of 120 °C and recovery of IL and P123 templates are the main advantages of this method. The disadvantages of this method might be the challenging synthesis route, potential toxicity, high cost, and required purification.

3. CHALLENGES AND PERSPECTIVES

Mesoporous silica materials have attracted a lot of attention in recent decades due to their highly tunable textural and chemical characteristics, and they have been used as adsorbents and catalyst supports in a range of applications. Template removal is the most important and last step in the preparation of mesoporous silica materials, and it has a great effect on the final properties of desired materials. Calcination under an air atmosphere at a high temperature of 550 °C for more than 5 h is the common method to obtain porosity. Despite its great effectiveness at removing templates, calcination has several drawbacks, including structural shrinkage, reduced silanol concentrations, production of huge volumes of CO_2, and the inability to recover or reuse expensive organic templates. Many efforts have been reported in the literature to develop alternative methods to calcination. Herein, we have reviewed the developed approaches to remove various types of templates, as shown in Table 4. The advantages and disadvantages of template removal methods are presented in Table 4. Most of these methods are effective to remove the template from the pores by preserving high silanol density with less shrinkage and possibly a higher micropore volume. However, due to the inability to recover or reuse the template, CO_2 emissions at the end of the process, and particularly the requirement of a complicated and expensive apparatus for template removal, it is unlikely that these developed technologies will be used on a large scale in the next years.

To remove the template from nonfunctionalized mesoporous silica materials, calcination is a preferred option in the laboratory regardless of its disadvantages. For many desired applications, mesoporous silica materials are functionalized with organic groups, for example, an amino group, via grafting and co-condensation methods. In such cases, calcination is no longer an option due to the elimination of the functional group along with the template, and the template is usually removed using a solvent extraction technique to preserve functional

https://doi.org/10.1021/acs.energyfuels.1c04435
Energy Fuels XXXX, XXX, XXX−XXX

Table 4. Comparing Different Template Removal Methods

Template removal method	Advantages	Disadvantages	ref
		Physical method	
Calcination	Highly template removal efficiency	Conducting at high temperature, significant framework shrinkage, reduction of silanol concentrations, generation of large amounts of CO_2 and toxic gases, and inability to recover or reuse templates	33−39
SC−CO_2 extraction	High template removal efficiency in the presence of solvents, preserving high silanol concentration, and possible recovery or reuse of template	Equipment limitation, using cosolvents to enhance template removal efficiency, and difficulties to achieve the appropriate temperature, pressure, and CO_2 flow speed	35, 36, 43−47
Microwave-assisted treatment	High template removal efficiency, quick template removal, less energy consumption, and less framework shrinkage	Emission of CO_2 and toxic gases, inability to recover or reuse the surfactant, use of solvents for assisting the template removal process, and equipment limitation	49, 50
Ultrasonic-assisted treatment	High template removal efficiency, preserving high silanol concentration, less framework shrinkage, and possible recovery or reuse of template	Ineffective to remove the template completely at low temperature in some cases, and required organic solvents	60−62
Ozone treatment	High template removal efficiency and less carbon content	Emission of CO_2 and toxic gases, longer reaction time in some cases, equipment limitation, and inability to recover or reuse the surfactant	52, 68−70
Plasma technology	High template removal efficiency, operation under ambient conditions, preserving high silanol concentration, less framework shrinkage, and less exposure time	Emission of CO_2 and toxic gases, inability to recover or reuse the surfactant, equipment limitation, inability to recover or reuse the surfactant, higher carbon content compared to calcination, required greater electrical voltage, and deposition of solid byproducts on the reactor's inner surface and electrodes	74−80
		Chemical methods	
Solvent extraction	Preserving high silanol concentration, less framework shrinkage, and possible recovery or reuse of template	Less template removal efficiency and large volume consumption of organic solvent	106−118
Chemical oxidation	High template removal efficiency, high silanol concentration, and less framework shrinkage	Longer reaction time, the existence of metal ions in the framework (if Fenton reagents used), generation of CO_2, and inability to recover or reuse the surfactant	108, 135, 138−141
IL treatment	High template removal efficiency, high concentration of surface silanols, less framework shrinkage, required a low temperature of 120 °C, and possible recovery of template	Challenging synthesis route, potential toxicity, high cost, and required purification	145

https://doi.org/10.1021/acs.energyfuels.1c04435
Energy Fuels XXXX, XXX, XXX−XXX

groups. Despite the fact that the process and apparatus are simple and the template might be recovered, removing the template through the solvent extraction approach is not good enough and requires a large amount of solvent and a lengthy time, so it is not the preferred method from environmental and economical perspectives.

For high template removal efficiency and a high silanol density, a combination of two or three methods is frequently utilized instead of high-temperature calcination alone. For instance, the template is removed first via solvent extraction and then calcination at a low temperature. The combination approach, on the other hand, comes at an additional expense and takes longer.

Because of several advantages such as ease of use, high template removal efficiency, less framework shrinkage, maintaining a high silanol density on the surface, template recovery, and no equipment limitations, we believe that IL treatment could be considered a potential approach for template removal. But still, some questions need to be answered, such as whether IL can effectively remove various types of surfactants (nonionic, cationic, and anionic) from various mesoporous silica materials. Furthermore, the template removal conditions need to be optimized by studying various factors such as, for example, solid to liquid ratio of the sample/IL, temperature, reaction time, ane stirring rate.

Despite the fact that there is relatively little evidence in the literature, IL treatment may attract researchers' interests in the near future. But, bearing in mind that ILs suffer several disadvantages including potential toxicity, the creation of large amounts of waste, availability and cost issues, purification and complex reaction steps, poor biodegradability, and high viscosity which may limit their use in large-scale industrial applications, it is essential to find promising solvents as alternatives to IL for template removal.

Deep eutectic solvents (DESs), also known as IL analogues, have emerged as possible alternatives to ILs. DESs are composed of two or more components, namely, hydrogen bond acceptor (HBA) and hydrogen bond donor (HBD), which can associate with each other through hydrogen bonding interactions.[103,146−158] DESs share the same properties as ILs but enjoy several advantages over ILs: (1) They can be used without purification. (2) Their preparation is easy. (3) They have low cost, good renewability, and low toxicity.

Many types of ILs and DESs have been utilized for biomass delignifcation which are effective to break hydrogen bonds within the cellulose. Among DESs, acid-based DES, base DES, polyalocohol-based DES, and phenolic-based DES have been used for biomass delignifcation.[159,160] Among these DESs, choline chloride-oxalic acid (1:1) showed an excellent performance to remove lignin. As reported by Zhang et al.,[161] biomass pretreatment with acid-based DESs such as choline chloride (ChCl)-oxalic acid (Ox) (1:1) removed 98.5% of lignin by stirring at 90 °C for 24 h. Moreover, their results showed that polyalocohol-based DES, ChCl-ethylene glycol (EG) (1:2), can remove about 87.6% of the lignin from corncob biomass. Also, the performance of IL or DES treatment in template removal is the same as that in biomass delignifcation. The DES can break the hydrogen bonding between hydroxyl groups on the surface of virgin mesoporous silica materials and the template at a low temperature leading to retaining a high silanol density on the surface as well. Due to the tunable properties of DESs, it is possible to prepare task-specific DES or ternary DES to enhance template removal efficiency. Therefore, as an alternative to IL treatment and future works, DES treatment is proposed for template removal from mesoporous silica materials.

4. CONCLUSIONS

Template removal is a crucial step in the synthesis of mesoporous silica materials. In the present study, we have discussed several methods to remove a variety of templates such as nonionic, cationic, and anionic surfactants as well as IL from different types of mesoporous silica materials. Among physical and chemical methods discussed here, calcination and solvent extortion methods are widely used for template removal. However, it is frequently noted that thermal calcination at high temperatures for many hours has some drawbacks, including framework shrinkage, lower silanol content, and the burning off of costly templates, which results in CO_2 and hazardous gas emissions. The latter method also necessitates a large volume of solvent and a long time, and it is inefficient in effectively removing the template. Therefore, to mitigate the problems related to conventional methods, many physical and chemical methods have been utilized for template removal. The literature survey indicates that the majority of the developed methods can efficiently remove templates while preserving the high silanol content at mild conditions. However, when these new methods for template removal were implemented, certain major issues remained that may limit their practical applicability: (1) Costly templates cannot be recovered or reused. (2) CO_2 and hazardous gas are produced at the end of the process. (3) The equipment has limitations. Among the developed methods, IL treatment showed an excellent performance in template removal without suffering the above-mentioned problems.

AUTHOR INFORMATION

Corresponding Author

Ming Zhao − *School of Environment, Tsinghua University, Beijing 100084, China; Research Institute for Environmental Innovation (Suzhou), Tsinghua, Suzhou 215263, China;* orcid.org/0000-0002-5801-5593; Phone: +861062784701; Email: ming.zhao@tsinghua.edu.cn

Author

Hosein Ghaedi − *School of Environment, Tsinghua University, Beijing 100084, China*

Complete contact information is available at: https://pubs.acs.org/10.1021/acs.energyfuels.1c04435

Notes

The authors declare no competing financial interest.

Biographies

Hosein Ghaedi was born in the Iranian city of Chahvarz in the province of Fars in the year 1984. He is a Ph.D. candidate in Environmental Science and Engineering at Tsinghua University's School of Environment (Beijing, China), where he is supervised by Prof. Ming Zhao. He earned his M.Sc. in Chemical Engineering from Malaysia's Universiti Teknologi Petronas (UTP). His study focuses on utilizing deep eutectic solvents toward green synthesis and functionalization of mesoporous silica materials for CO_2 capture.

Dr. Ming Zhao is an Associate Professor of the School of Environment, Tsinghua University. He is the founder of the LBC Group (**L**ab for **B**io-resource & **C**arbon-mitigation Technologies). He

https://doi.org/10.1021/acs.energyfuels.1c04435
Energy Fuels XXXX, XXX, XXX−XXX

obtained his Ph.D. in Chemical Engineering from the University of Sydney in 2010. He joined Tsinghua University after the completion of his work at the Imperial College London in 2014. Dr. Zhao and his group possess expertise in thermo-chemical conversion of biomass (wastes) into clean energy and value-added chemicals and CO_2 capture and utilization. The LBC Group has published 90+ peer-reviewed articles in recent years. Dr. Zhao also maintains linkage to the industry, and one of his gasification technologies has been commercialized for gaseous fuel production from solid wastes.

■ ACKNOWLEDGMENTS

Hosein Ghaedi and Ming Zhao are grateful for the support of the National Key Research and Development Program of China (2018YFC1901300).

■ ABBREVIATION DEFINITION

SBA	Santa Barbara Amorphous
MCM	Mobil Composition of Matter
KIT	Korean Advanced Institute of Science and Technology
ZSM-5	Zeolite Socony Mobil-5
P123	Poly(ethylene glycol)-*block*-poly(propylene glycol)-*block*-poly(ethylene glycol)
F-127	Poly(ethylene oxide)-poly(propylene oxide)-poly(ethylene oxide)
CTABr	Cetyltrimethylammonium bromide
CTEABr	Cetyltriethylammonium bromide
SDBS	Sodium dodecyl benzenesulfonate
SDS	Sodium dodecyl sulfate
LAS	Lauric acid sodium
TEOS	Tetraethyl orthosilicate
PhTES	Phenyltriethoxysilane
APS	Aminopropyltriethoxysilane
CES	Carboxyethylsilanetriol sodium salt
$HO^{\bullet}$	Hydroxyl radicals
UV	Ultraviolet
SCF	Supercritical fluid
SC−CO_2	Suppercritical CO_2
BJH	Barett−Joyner−Halenda
HCl	Hydrochloric acid
H_2SO_4	Sulfuric acid
HNO_3	Nitric acid
$PrSO_3H$	Propylsulfonic acid
H_2O_2	Hydrogen peroxide
DMSO	Dimethyl sulfoxide
$KMnO_4$	Potassium permanganate
IL	Ionic liquid
$[C_4mim]Cl$	1-Butyl-3-methylimidazolium chloride
$[C_4mim]BF_4$	1-Butyl-3-methyl-imidazolium-tetrafluoroborate
THF	Tetrahydrofuran
VOC	Volatile organic compound
V_T	Total pore volume
S_{BET}	BET specific surface area
a_0	Unit cell parameter
NMR	Nuclear magnetic resonance
SAXRD	Small-angle X-ray diffraction
FT-IR	Fourier transform infrared spectroscopy
SEM	Scanning electron microscope
TEM	Transmission electron microscopy
TGA	Thermogravimetric analysis
GC-MS	Gas chromatography−mass spectrometry
NTP	Nonthermal plasma
DBD	Dielectric barrier discharge
SDBD	Single dielectric-barrier discharge
DDBD	Double dielectric-barrier discharge
GD	Glow discharge

■ REFERENCES

(1) Jafari, S.; Derakhshankhah, H.; Alaei, L.; Fattahi, A.; Varnamkhasti, B. S.; Saboury, A. A. Mesoporous silica nanoparticles for therapeutic/diagnostic applications. *Biomedicine & Pharmacotherapy* **2019**, *109*, 1100−1111.

(2) Rahikkala, A.; Pereira, S. A. P.; Figueiredo, P.; Passos, M. L. C.; Araújo, A. R. T. S.; Saraiva, M. L. M. F. S.; Santos, H. A. Mesoporous Silica Nanoparticles for Targeted and Stimuli-Responsive Delivery of Chemotherapeutics: A Review. *Advanced Biosystems* **2018**, *2* (7), 1800020.

(3) Nguyen, T. L.; Choi, Y.; Kim, J. Mesoporous Silica as a Versatile Platform for Cancer Immunotherapy. *Adv. Mater.* **2019**, *31* (34), 1803953.

(4) Dinker, M. K.; Kulkarni, P. S. Recent Advances in Silica-Based Materials for the Removal of Hexavalent Chromium: A Review. *Journal of Chemical & Engineering Data* **2015**, *60* (9), 2521−2540.

(5) Cashin, V. B.; Eldridge, D. S.; Yu, A.; Zhao, D. Surface functionalization and manipulation of mesoporous silica adsorbents for improved removal of pollutants: a review. *Environmental Science: Water Research & Technology* **2018**, *4* (2), 110−128.

(6) Liang, J.; Liang, Z.; Zou, R.; Zhao, Y. Heterogeneous Catalysis in Zeolites, Mesoporous Silica, and Metal−Organic Frameworks. *Adv. Mater.* **2017**, *29* (30), 1701139.

(7) Wang, F.; Jiang, L.; Wang, J.; Zhang, Z. Catalytic Conversion of Fructose and 5-Hydroxymethylfurfural into 2,5-Diformylfuran over SBA-15 Supported Ruthenium Catalysts. *Energy Fuels* **2016**, *30* (7), 5885−5892.

(8) Wang, L.; Diao, Z.; Tian, Y.; Xiong, Z.; Liu, G. Catalytic Cracking of Endothermic Hydrocarbon Fuels over Ordered Meso-HZSM-5 Zeolites with Al-MCM-41 Shells. *Energy Fuels* **2016**, *30* (9), 6977−6983.

(9) Perumal, T.; Mangesh, V. L.; Perumal, S. K.; Arumugam, R.; Subramanian, N.; Subramanian, S.; Kannan, S. Isomerization of Alkanes over Ionic Liquids Supported on SBA-15. *Energy Fuels* **2020**, *34* (11), 14620−14632.

(10) Lv, Y.; Wang, X.; Gao, D.; Ma, X.; Li, S.; Wang, Y.; Song, G.; Duan, A.; Chen, G. Hierarchically Porous ZSM-5/SBA-15 Zeolite: Tuning Pore Structure and Acidity for Enhanced Hydro-Upgrading of FCC Gasoline. *Ind. Eng. Chem. Res.* **2018**, *57* (42), 14031−14043.

(11) Mulu, E.; M'Arimi, M. M.; Ramkat, R. C. A review of recent developments in application of low cost natural materials in purification and upgrade of biogas. *Renewable and Sustainable Energy Reviews* **2021**, *145*, 111081.

(12) Melde, B. J.; Johnson, B. J.; Charles, P. T. Mesoporous Silicate Materials in Sensing. *Sensors* **2008**, *8* (8), 5202.

(13) Méndez, F. J.; Franco-López, O. E.; Bokhimi, X.; Solís-Casados, D. A.; Escobar-Alarcón, L.; Klimova, T. E. Dibenzothiophene hydrodesulfurization with NiMo and CoMo catalysts supported on niobium-modified MCM-41. *Applied Catalysis B: Environmental* **2017**, *219*, 479−491.

(14) Tanimu, A.; Abdel-Azeim, S.; Ganiyu, S. A.; Alhooshani, K. Experimental and Theoretical Investigation of the Synergy Effect of Zr and Ce on the Catalytic Efficiency of NiMoS Grafted on SBA-15 for Oil Hydrodesulfurization. *Energy Fuels* **2021**, *35* (3), 2579−2589.

(15) Wang, X.; Shi, Y.; Gao, S.; Xu, C.; Zhao, Z.; Wang, G.; Fu, S.; Duan, A.; Gao, D. Hierarchically Porous β/SBA-16 Composites: Tuning Pore Structure and Acidity for Enhanced Isomerization Performance in Hydrodesulfurization of Dibenzothiophene and 4,6-Dimethyldibenzothiophene. *Energy Fuels* **2020**, *34* (1), 769−777.

(16) Ganiyu, S. A.; Alhooshani, K. Catalytic Performance of NiMoS Supported on (Zr)SBA-15 for Hydrodesulfurization of Diesel: Insight into a One-Step Calcination and Reduction Strategy during Sulfidation. *Energy Fuels* **2019**, *33* (4), 3047−3056.

https://doi.org/10.1021/acs.energyfuels.1c04435
Energy Fuels XXXX, XXX, XXX−XXX

(17) Zheng, P.; Hu, D.; Meng, Q.; Liu, C.; Wang, X.; Fan, J.; Duan, A.; Xu, C. Influence of Support Acidity on the HDS Performance over β-SBA-16 and Al-SBA-16 Substrates: A Combined Experimental and Theoretical Study. *Energy Fuels* **2019**, *33* (2), 1479−1488.
(18) Wu, M.; Li, Q.; Wang, X.; Mi, J. Structure Characteristics and Hot-Coal-Gas Desulfurization Properties of Zn-Based Sorbents Supported on Mesoporous Silica with Different Pore-Arrangement Patterns: A Comparison Study. *Energy Fuels* **2021**, *35* (3), 2456−2467.
(19) Akopyan, A.; Polikarpova, P.; Gul, O.; Anisimov, A.; Karakhanov, E. Catalysts Based on Acidic SBA-15 for Deep Oxidative Desulfurization of Model Fuels. *Energy Fuels* **2020**, *34* (11), 14611−14619.
(20) Polikarpova, P.; Akopyan, A.; Shigapova, A.; Glotov, A.; Anisimov, A.; Karakhanov, E. Oxidative Desulfurization of Fuels Using Heterogeneous Catalysts Based on MCM-41. *Energy Fuels* **2018**, *32* (10), 10898−10903.
(21) Rao, N.; Wang, M.; Shang, Z.; Hou, Y.; Fan, G.; Li, J. CO2 Adsorption by Amine-Functionalized MCM-41: A Comparison between Impregnation and Grafting Modification Methods. *Energy Fuels* **2018**, *32* (1), 670−677.
(22) Kishor, R.; Ghoshal, A. K. Polyethylenimine Functionalized As-Synthesized KIT-6 Adsorbent for Highly CO2/N2 Selective Separation. *Energy Fuels* **2016**, *30* (11), 9635−9644.
(23) Du, H.; Ma, L.; Liu, X.; Zhang, F.; Yang, X.; Wu, Y.; Zhang, J. A Novel Mesoporous SiO2Material with MCM-41 Structure from Coal Gangue: Preparation, Ethylenediamine Modification, and Adsorption Properties for CO2 Capture. *Energy Fuels* **2018**, *32* (4), 5374−5385.
(24) Chen, H.; Liang, Z.; Yang, X.; Zhang, Z.; Zhang, Z. Experimental Investigation of CO2 Capture Capacity: Exploring Mesoporous Silica SBA-15 Material Impregnated with Monoethanolamine and Diethanolamine. *Energy Fuels* **2016**, *30* (11), 9554−9562.
(25) Ye, C.-P.; Wang, R.-N.; Gao, X.; Li, W.-Y. CO2 Capture Performance of Supported Phosphonium Dual Amine-Functionalized Ionic Liquids@MCM-41. *Energy Fuels* **2020**, *34* (11), 14379−14387.
(26) Zhang, W.; Li, Y.; Li, Y.; Gao, E.; Cao, G.; Bernards, M. T.; He, Y.; Shi, Y. Enhanced SO2 Resistance of Tetraethylenepentammonium Nitrate Protic Ionic Liquid-Functionalized SBA-15 during CO2 Capture from Flue Gas. *Energy Fuels* **2020**, *34* (7), 8628−8634.
(27) Zhang, W.; Gao, E.; Li, Y.; Bernards, M. T.; Li, Y.; Cao, G.; He, Y.; Shi, Y. Synergistic Enhancement of CO2 Adsorption Capacity and Kinetics in Triethylenetetrammonium Nitrate Protic Ionic Liquid Functionalized SBA-15. *Energy Fuels* **2019**, *33* (9), 8967−8975.
(28) Venkateshwaran, S.; Partheeban, T.; Sasidharan, M.; Senthil Kumar, S. M. Mesoporous Silica Template-Assisted Synthesis of 1T-MoS2 as the Anode for Li-Ion Battery Applications. *Energy Fuels* **2021**, *35* (3), 2683−2691.
(29) Subagyono, R. R. D. J. N.; Marshall, M.; Jackson, W. R.; Auxilio, A. R.; Fei, Y.; Chaffee, A. L. Upgrading Microalgal Biocrude Using NiMo/Al-SBA-15 as a Catalyst. *Energy Fuels* **2020**, *34* (4), 4618−4631.
(30) Meng, Q.; Duan, A.; Chi, K.; Zhao, Z.; Liu, J.; Zheng, P.; Wang, B.; Liu, C.; Hu, D.; Jia, Y. Synthesis of Titanium Modified Three-Dimensional KIT-5 Mesoporous Support and Its Application of the Quinoline Hydrodenitrogenation. *Energy Fuels* **2019**, *33* (6), 5518−5528.
(31) Gutta, N.; Velisoju, V. K.; Tardio, J.; Patel, J.; Satyanarayana, L.; Sarma, A. V. S.; Akula, V. CH4 Cracking over the Cu−Ni/Al-MCM-41 Catalyst for the Simultaneous Production of H2 and Highly Ordered Graphitic Carbon Nanofibers. *Energy Fuels* **2019**, *33* (12), 12656−12665.
(32) Gutta, N.; Velisoju, V. K.; Chatla, A.; Boosa, V.; Tardio, J.; Patel, J.; Akula, V. Promotional Effect of Cu and Influence of Surface Ni−Cu Alloy for Enhanced H2 Yields from CH4 Decomposition over Cu-Modified Ni Supported on MCM-41 Catalyst. *Energy Fuels* **2018**, *32* (3), 4008−4015.
(33) Hung, C.; Bai, H.; Karthik, M. Ordered mesoporous silica particles and Si-MCM-41 for the adsorption of acetone: A comparative study. *Sep. Purif. Technol.* **2009**, *64* (3), 265−272.
(34) Basso, A. M.; Nicola, B. P.; Bernardo-Gusmão, K.; Pergher, S. B. C. Tunable Effect of the Calcination of the Silanol Groups of KIT-6 and SBA-15 Mesoporous Materials. *Applied Sciences* **2020**, *10* (3), 970.
(35) Huang, L.; Kawi, S.; Poh, C.; Hidajat, K.; Ng, S. C. Extraction of cationic surfactant templates from mesoporous materials by CH3OH-modified CO2 supercritical fluid. *Talanta* **2005**, *66* (4), 943−951.
(36) Huang, Z.; Huang, L.; Shen, S. C.; Poh, C. C.; Hidajat, K.; Kawi, S.; Ng, S. C. High quality mesoporous materials prepared by supercritical fluid extraction: effect of curing treatment on their structural stability. *Microporous Mesoporous Mater.* **2005**, *80* (1), 157−163.
(37) Krawiec, P.; Kockrick, E.; Simon, P.; Auffermann, G.; Kaskel, S. Platinum-Catalyzed Template Removal for the in Situ Synthesis of MCM-41 Supported Catalysts. *Chem. Mater.* **2006**, *18* (11), 2663−2669.
(38) Zaleski, R.; Wawryszczuk, J.; Borówka, A.; Goworek, J.; Goworek, T. Temperature changes of the template structure in MCM-41 type materials; positron annihilation studies. *Microporous Mesoporous Mater.* **2003**, *62* (1), 47−60.
(39) Ryczkowski, J.; Goworek, J.; Gac, W.; Pasieczna, S.; Borowiecki, T. Temperature removal of templating agent from MCM-41 silica materials. *Thermochim. Acta* **2005**, *434* (1), 2−8.
(40) Goworek, J.; Kierys, A.; Kusak, R. Isothermal template removal from MCM-41 in hydrogen flow. *Microporous Mesoporous Mater.* **2007**, *98* (1), 242−248.
(41) Camel, V.; Tambuté, A.; Caude, M. Analytical-scale supercritical fluid extraction: a promising technique for the determination of pollutants in environmental matrices. *J. Chromatogr. A* **1993**, *642* (1), 263−281.
(42) Hawthorne, S. B. Analytical-scale supercritical fluid extraction. *Anal. Chem.* **1990**, *62* (11), 633A−642A.
(43) Huang, Z.; Luan, D. Y.; Shen, S. C.; Hidajat, K.; Kawi, S. Supercritical fluid extraction of the organic template from synthesized porous materials: effect of pore size. *Journal of Supercritical Fluids* **2005**, *35* (1), 40−48.
(44) Lu, X.-B.; Zhang, W.-H.; Xiu, J.-H.; He, R.; Chen, L.-G.; Li, X. Removal of the Template Molecules from MCM-41 with Supercritical Fluid in a Flow Apparatus. *Ind. Eng. Chem. Res.* **2003**, *42* (3), 653−656.
(45) van Grieken, R.; Calleja, G.; Stucky, G. D.; Melero, J. A.; García, R. A.; Iglesias, J. Supercritical Fluid Extraction of a Nonionic Surfactant Template from SBA-15 Materials and Consequences on the Porous Structure. *Langmuir* **2003**, *19* (9), 3966−3973.
(46) Huang, Z.; Li, J.-h.; Li, H.-s.; Teng, L.-j.; Kawi, S.; Lai, M. W. Effects of polar modifiers on supercritical extraction efficiency for organic template removal from mesoporous MCM-41 materials. The. *J. Supercrit. Fluids* **2013**, *82*, 96−105.
(47) Huang, Z.; Xu, L.; Li, J.-H.; Kawi, S.; Goh, A. H. Organic template removal from hexagonal mesoporous silica by means of methanol-enhanced CO2 extraction: Effect of temperature, pressure and flow rate. *Sep. Purif. Technol.* **2011**, *77* (1), 112−119.
(48) Chen, L.; Jiang, S.; Wang, R.; Zhang, Z.; Qiu, S. A novel, efficient and facile method for the template removal from mesoporous materials. *Chemical Research in Chinese Universities* **2014**, *30* (6), 894−899.
(49) Tian, B.; Liu, X.; Yu, C.; Gao, F.; Luo, Q.; Xie, S.; Tu, B.; Zhao, D. Microwave assisted template removal of siliceous porous materials. *Chem. Commun.* **2002**, No. 11, 1186−1187.
(50) Lai, T.-L.; Shu, Y.-Y.; Lin, Y.-C.; Chen, W.-N.; Wang, C.-B. Rapid removal of organic template from SBA-15 with microwave assisted extraction. *Mater. Lett.* **2009**, *63* (20), 1693−1695.
(51) Li, X.; Yin, H.; Zhang, J.; Liu, J.; Chen, G. Effect of organic template removal approaches on physiochemical characterization of Ni/Al-SBA-15 and eugenol hydrodeoxygenation. *J. Solid State Chem.* **2020**, *282*, 121063.
(52) López-Pérez, L.; López-Martínez, M.-A.; Djanashvili, K.; Góra-Marek, K.; Tarach, K. A.; Borges, M. E.; Melián-Cabrera, I. Process

https://doi.org/10.1021/acs.energyfuels.1c04435
Energy Fuels XXXX, XXX, XXX−XXX

Intensification of Mesoporous Material's Synthesis by Microwave-Assisted Surfactant Removal. *ACS Sustainable Chem. Eng.* **2020**, *8* (45), 16814−16822.
(53) Qiao, S. Z.; Liu, J.; Max Lu, G. Q. Chapter 21 - Synthetic Chemistry of Nanomaterials. In *Modern Inorganic Synthetic Chemistry*, Second ed.; Xu, R.; Xu, Y., Eds.; Elsevier: Amsterdam, 2017; pp 613−640.
(54) Perelshtein, I.; Perkas, N.; Gedanken, A. Chapter 3 - Making the Hospital a Safer Place by the Sonochemical Coating of Textiles by Antibacterial Nanoparticles. In *Surface Chemistry of Nanobiomaterials*; Grumezescu, A. M., Ed.; William Andrew Publishing, 2016; pp 71−105.
(55) Suslick, K. S.; Hammerton, D. A.; Cline, R. E. Sonochemical hot spot. *J. Am. Chem. Soc.* **1986**, *108* (18), 5641−5642.
(56) Moradi, E.; Rahimi, R.; Safarifard, V. Sonochemically synthesized microporous metal−organic framework representing unique selectivity for detection of Fe3+ ions. *Polyhedron* **2019**, *159*, 251−258.
(57) Bang, J. H.; Suslick, K. S. Applications of Ultrasound to the Synthesis of Nanostructured Materials. *Adv. Mater.* **2010**, *22* (10), 1039−1059.
(58) Hinman, J. J.; Suslick, K. S., Nanostructured Materials Synthesis Using Ultrasound. In *Sonochemistry: From Basic Principles to Innovative Applications*; Colmenares, J. C., Chatel, G., Eds.; Springer International Publishing: Cham, 2017; pp 59−94.
(59) Xu, H.; Zeiger, B. W.; Suslick, K. S. Sonochemical synthesis of nanomaterials. *Chem. Soc. Rev.* **2013**, *42* (7), 2555−2567.
(60) Jabariyan, S.; Zanjanchi, M. A. A simple and fast sonication procedure to remove surfactant templates from mesoporous MCM-41. *Ultrason. Sonochem.* **2012**, *19* (5), 1087−1093.
(61) Zanjanchi, M. A.; Jabariyan, S. Application of ultrasound and methanol for rapid removal of surfactant from MCM-41. *J. Serb. Chem. Soc.* **2014**, *79* (1), 25−38.
(62) Pirez, C.; Wilson, K.; Lee, A. F. An energy-efficient route to the rapid synthesis of organically-modified SBA-15 via ultrasonic template removal. *Green Chem.* **2014**, *16* (1), 197−202.
(63) Li, F.; Xie, C.; Cheng, Z.; Xia, H. Ultrasound responsive block copolymer micelle of poly(ethylene glycol)−poly(propylene glycol) obtained through click reaction. *Ultrason. Sonochem.* **2016**, *30*, 9−17.
(64) Husseini, G. A.; Pitt, W. G. Micelles and nanoparticles for ultrasonic drug and gene delivery. *Adv. Drug Delivery Rev.* **2008**, *60* (10), 1137−1152.
(65) Xuan, J.; Pelletier, M.; Xia, H.; Zhao, Y. Ultrasound-Induced Disruption of Amphiphilic Block Copolymer Micelles. *Macromol. Chem. Phys.* **2011**, *212* (5), 498−506.
(66) Hozumi, A.; Yokogawa, Y.; Kameyama, T.; Hiraku, K.; Sugimura, H.; Takai, O.; Okido, M. Photocalcination of Mesoporous Silica Films Using Vacuum Ultraviolet Light. *Adv. Mater.* **2000**, *12* (13), 985−987.
(67) Ha, C.-S.; Park, S. S. General Synthesis and Physico-chemical Properties of Mesoporous Materials. In *Periodic Mesoporous Organosilicas: Preparation, Properties and Applications*; Ha, C.-S.; Park, S. S., Eds.; Springer Singapore: Singapore, 2019; pp 15−85.
(68) Keene, M. T. J.; Denoyel, R.; Llewellyn, P. L. Ozone treatment for the removal of surfactant to form MCM-41 type materials. *Chem. Commun.* **1998**, *20*, 2203−2204.
(69) Büchel, G.; Denoyel, R.; Llewellyn, P. L.; Rouquerol, J. In situ surfactant removal from MCM-type mesostructures by ozone treatment. *J. Mater. Chem.* **2001**, *11* (2), 589−593.
(70) Joshi, H.; Jalalpoor, D.; Ochoa-Hernández, C.; Schmidt, W.; Schüth, F. Ozone Treatment: A Versatile Tool for the Postsynthesis Modification of Porous Silica-Based Materials. *Chem. Mater.* **2018**, *30* (24), 8905−8914.
(71) Vogna, D.; Marotta, R.; Napolitano, A.; d'Ischia, M. Advanced Oxidation Chemistry of Paracetamol. UV/H2O2-Induced Hydroxylation/Degradation Pathways and 15N-Aided Inventory of Nitrogenous Breakdown Products. The. *J. Org. Chem.* **2002**, *67* (17), 6143−6151.
(72) Cater, S. R.; Stefan, M. I.; Bolton, J. R.; Safarzadeh-Amiri, A. UV/H2O2 Treatment of Methyl tert-Butyl Ether in Contaminated Waters. *Environ. Sci. Technol.* **2000**, *34* (4), 659−662.
(73) Xiao, L.; Li, J.; Jin, H.; Xu, R. Removal of organic templates from mesoporous SBA-15 at room temperature using UV/dilute H2O2. *Microporous Mesoporous Mater.* **2006**, *96* (1), 413−418.
(74) Aumond, T.; Pinard, L.; Batiot-Dupeyrat, C.; Sachse, A. Non-thermal plasma: A fast and efficient template removal approach allowing for new insights to the SBA-15 structure. *Microporous Mesoporous Mater.* **2020**, *296*, 110015.
(75) Liu, Y.; Wang, Z.; Liu, C.-j. Mechanism of template removal for the synthesis of molecular sieves using dielectric barrier discharge. *Catal. Today* **2015**, *256*, 137−141.
(76) Liu, Y.; Pan, Y.; Wang, Z.-J.; Kuai, P.; Liu, C.-J. Facile and fast template removal from mesoporous MCM-41 molecular sieve using dielectric-barrier discharge plasma. *Catal. Commun.* **2010**, *11* (6), 551−554.
(77) Liu, Y.; Pan, Y.-x.; Kuai, P.; Liu, C.-j. Template Removal from ZSM-5 Zeolite Using Dielectric-Barrier Discharge Plasma. *Catal. Lett.* **2010**, *135* (3), 241−245.
(78) Yuan, M.-H.; Wang, L.; Yang, R. T. Glow Discharge Plasma-Assisted Template Removal of SBA-15 at Ambient Temperature for High Surface Area, High Silanol Density, and Enhanced CO2 Adsorption Capacity. *Langmuir* **2014**, *30* (27), 8124−8130.
(79) Maesen, T. L. M.; Kouwenhoven, H. W.; van Bekkum, H.; Sulikowski, B.; Klinowski, J. Template removal from molecular sieves by low-temperature plasma calcination. *J. Chem. Soc., Faraday Trans.* **1990**, *86* (23), 3967−3970.
(80) Wang, L.; Yao, J.; Wang, Z.; Jiao, H.; Qi, J.; Yong, X.; Liu, D. Fast and low-temperature elimination of organic templates from SBA-15 using dielectric barrier discharge plasma. *Plasma Science and Technology* **2018**, *20* (10), 101001.
(81) Khataee, A.; Sajjadi, S.; Hasanzadeh, A.; Vahid, B.; Joo, S. W. One-step preparation of nanostructured martite catalyst and graphite electrode by glow discharge plasma for heterogeneous electro-Fenton like process. *Journal of Environmental Management* **2017**, *199*, 31−45.
(82) Bazaka, K.; Baranov, O.; Cvelbar, U.; Podgornik, B.; Wang, Y.; Huang, S.; Xu, L.; Lim, J. W. M.; Levchenko, I.; Xu, S. Oxygen plasmas: a sharp chisel and handy trowel for nanofabrication. *Nanoscale* **2018**, *10* (37), 17494−17511.
(83) Wang, Z.-j.; Xie, Y.; Liu, C.-j. Synthesis and Characterization of Noble Metal (Pd, Pt, Au, Ag) Nanostructured Materials Confined in the Channels of Mesoporous SBA-15. *J. Phys. Chem. C* **2008**, *112* (50), 19818−19824.
(84) Mamdouh, W.; Li, Y.; Shawky, S. M.; Azzazy, H. M. E.; Liu, C.-J. Influence of "Glow Discharge Plasma" as an External Stimulus on the Self-Assembly, Morphology and Binding Affinity of Gold Nanoparticle-Streptavidin Conjugates. *International Journal of Molecular Sciences* **2012**, *13* (6), 6534.
(85) Guo, Q.; With, P.; Liu, Y.; Gläser, R.; Liu, C.-j. Carbon template removal by dielectric-barrier discharge plasma for the preparation of zirconia. *Catal. Today* **2013**, *211*, 156−161.
(86) Wang, B.; Chen, B.; Sun, Y.; Xiao, H.; Xu, X.; Fu, M.; Wu, J.; Chen, L.; Ye, D. Effects of dielectric barrier discharge plasma on the catalytic activity of Pt/CeO2 catalysts. *Applied Catalysis B: Environmental* **2018**, *238*, 328−338.
(87) Li, Y.; Wang, W.; Wang, F.; Di, L.; Yang, S.; Zhu, S.; Yao, Y.; Ma, C.; Dai, B.; Yu, F. Enhanced Photocatalytic Degradation of Organic Dyes via Defect-Rich TiO2 Prepared by Dielectric Barrier Discharge Plasma. *Nanomaterials* **2019**, *9* (5), 720.
(88) Das, P.; Ojah, N.; Kandimalla, R.; Mohan, K.; Gogoi, D.; Dolui, S. K.; Choudhury, A. J. Surface modification of electrospun PVA/chitosan nanofibers by dielectric barrier discharge plasma at atmospheric pressure and studies of their mechanical properties and biocompatibility. *Int. J. Biol. Macromol.* **2018**, *114*, 1026−1032.
(89) Xu, X. Dielectric barrier discharge — properties and applications. *Thin Solid Films* **2001**, *390* (1), 237−242.

https://doi.org/10.1021/acs.energyfuels.1c04435
Energy Fuels XXXX, XXX, XXX−XXX

(90) Hashim, S. A.; Samsudin, F. N. D. b.; Wong, C. S.; Abu Bakar, K.; Yap, S. L.; Mohd. Zin, M. F. Non-thermal plasma for air and water remediation. *Arch. Biochem. Biophys.* **2016**, *605*, 34−40.
(91) Zhang, C.; Sun, Y.; Yu, Z.; Zhang, G.; Feng, J. Simultaneous removal of Cr(VI) and acid orange 7 from water solution by dielectric barrier discharge plasma. *Chemosphere* **2018**, *191*, 527−536.
(92) Sang, W.; Cui, J.; Feng, Y.; Mei, L.; Zhang, Q.; Li, D.; Zhang, W. Degradation of aniline in aqueous solution by dielectric barrier discharge plasma: Mechanism and degradation pathways. *Chemosphere* **2019**, *223*, 416−424.
(93) Iervolino, G.; Vaiano, V.; Palma, V. Enhanced removal of water pollutants by dielectric barrier discharge non-thermal plasma reactor. *Sep. Purif. Technol.* **2019**, *215*, 155−162.
(94) Yuan, D.; Wang, Z.; He, Y.; Xie, S.; Lin, F.; Zhu, Y.; Cen, K. Ozone Production with Dielectric Barrier Discharge from Air: The Influence of Pulse Polarity. *Ozone: Science & Engineering* **2018**, *40* (6), 494−502.
(95) Zylka, P. Evaluation of Ozone Generation in Volume Spiral-Tubular Dielectric Barrier Discharge Source. *Energies* **2020**, *13* (5), 1199.
(96) Zeng, Y. X.; Wang, L.; Wu, C. F.; Wang, J. Q.; Shen, B. X.; Tu, X. Low temperature reforming of biogas over K-, Mg- and Ce-promoted Ni/Al2O3 catalysts for the production of hydrogen rich syngas: Understanding the plasma-catalytic synergy. *Applied Catalysis B: Environmental* **2018**, *224*, 469−478.
(97) Wang, Y.; Yu, F.; Zhu, M.; Ma, C.; Zhao, D.; Wang, C.; Zhou, A.; Dai, B.; Ji, J.; Guo, X. N-Doping of plasma exfoliated graphene oxide via dielectric barrier discharge plasma treatment for the oxygen reduction reaction. *Journal of Materials Chemistry A* **2018**, *6* (5), 2011−2017.
(98) Zhang, H.; Li, K.; Shu, C.; Lou, Z.; Sun, T.; Jia, J. Enhancement of styrene removal using a novel double-tube dielectric barrier discharge (DDBD) reactor. *Chem. Eng. J.* **2014**, *256*, 107−118.
(99) Mustafa, M. F.; Fu, X.; Liu, Y.; Abbas, Y.; Wang, H.; Lu, W. Volatile organic compounds (VOCs) removal in non-thermal plasma double dielectric barrier discharge reactor. *J. Hazard. Mater.* **2018**, *347*, 317−324.
(100) Abbas, Y.; Lu, W.; Wang, Q.; Dai, H.; Liu, Y.; Fu, X.; Pan, C.; Ghaedi, H.; Cheng, F.; Wang, H. Remediation of pyrene contaminated soil by double dielectric barrier discharge plasma technology: Performance optimization and evaluation. *Environ. Pollut.* **2020**, *260*, 113944.
(101) Mu, R.; Liu, Y.; Li, R.; Xue, G.; Ognier, S. Remediation of pyrene-contaminated soil by active species generated from flat-plate dielectric barrier discharge. *Chem. Eng. J.* **2016**, *296*, 356−365.
(102) Aggelopoulos, C. A.; Hatzisymeon, M.; Tataraki, D.; Rassias, G. Remediation of ciprofloxacin-contaminated soil by nanosecond pulsed dielectric barrier discharge plasma: Influencing factors and degradation mechanisms. *Chem. Eng. J.* **2020**, *393*, 124768.
(103) Ghaedi, H.; Ayoub, M.; Sufian, S.; Lal, B.; Uemura, Y. Thermal stability and FT-IR analysis of Phosphonium-based deep eutectic solvents with different hydrogen bond donors. *J. Mol. Liq.* **2017**, *242*, 395−403.
(104) Pootawang, P.; Saito, N.; Takai, O. Solution plasma for template removal in mesoporous silica: pH and discharge time varying characteristics. *Thin Solid Films* **2011**, *519* (20), 7030−7035.
(105) Pootawang, P.; Saito, N.; Takai, O. Solution Plasma Process for Template Removal in Mesoporous Silica Synthesis. *Jpn. J. Appl. Phys.* **2010**, *49* (12), 126202.
(106) Lu, B.; Kawamoto, K. A novel approach for synthesizing ordered mesoporous silica SBA-15. *Mater. Res. Bull.* **2012**, *47* (6), 1301−1305.
(107) de Ávila, S. G.; Silva, L. C. C.; Matos, J. R. Optimisation of SBA-15 properties using Soxhlet solvent extraction for template removal. *Microporous Mesoporous Mater.* **2016**, *234*, 277−286.
(108) Barczak, M. Template removal from mesoporous silicas using different methods as a tool for adjusting their properties. *New J. Chem.* **2018**, *42* (6), 4182−4191.
(109) Gao, F.; Lu, Q.; Liu, X.; Yan, Y.; Zhao, D. Controlled Synthesis of Semiconductor PbS Nanocrystals and Nanowires Inside Mesoporous Silica SBA-15 Phase. *Nano Lett.* **2001**, *1* (12), 743−748.
(110) Aguado, J.; Arsuaga, J. M.; Arencibia, A.; Lindo, M.; Gascón, V. Aqueous heavy metals removal by adsorption on amine-functionalized mesoporous silica. *J. Hazard. Mater.* **2009**, *163* (1), 213−221.
(111) Lu, F.; Wu, S.-H.; Hung, Y.; Mou, C.-Y. Size Effect on Cell Uptake in Well-Suspended, Uniform Mesoporous Silica Nanoparticles. *Small* **2009**, *5* (12), 1408−1413.
(112) Laghaei, M.; Sadeghi, M.; Ghalei, B.; Dinari, M. The effect of various types of post-synthetic modifications on the structure and properties of MCM-41 mesoporous silica. *Prog. Org. Coat.* **2016**, *90*, 163−170.
(113) Cheng, S.; Wang, X.; Chen, S.-Y. Applications of Amine-functionalized Mesoporous Silica in Fine Chemical Synthesis. *Top. Catal.* **2009**, *52* (6), 681−687.
(114) Gokulakrishnan, N.; Karbowiak, T.; Bellat, J. P.; Vonna, L.; Saada, M.-A.; Paillaud, J. L.; Soulard, M.; Patarin, J.; Parmentier, J. Improved hydrophobicity of inorganic−organic hybrid mesoporous silica with cage-like pores. *Colloids Surf., A* **2013**, *421*, 34−43.
(115) Gao, J.; Wu, S.; Tan, F.; Tian, H.; Liu, J.; Lu, G. Q. M. Nanoengineering of amino - functionalized mesoporous silica nanospheres as nanoreactors. *Progress in Natural Science: Materials International* **2018**, *28* (2), 242−245.
(116) Wang, J.; Zheng, S.; Liu, J.; Xu, Z. Tannic acid adsorption on amino-functionalized magnetic mesoporous silica. *Chem. Eng. J.* **2010**, *165* (1), 10−16.
(117) Ghorbani, M.; Nowee, S. M.; Ramezanian, N.; Raji, F. A new nanostructured material amino functionalized mesoporous silica synthesized via co-condensation method for Pb(II) and Ni(II) ion sorption from aqueous solution. *Hydrometallurgy* **2016**, *161*, 117−126.
(118) Wu, H.-C.; Chen, T.-C.; Budi, C. S.; Huang, P.-H.; Chen, C.-S.; Kao, H.-M. Confinement of Pt nanoparticles in cage-type mesoporous silica SBA-16 as efficient catalysts for toluene oxidation: the effect of carboxylic groups on the mesopore surface. *Catalysis Science & Technology* **2019**, *9* (24), 6852−6862.
(119) Suteewong, T.; Sai, H.; Lee, J.; Bradbury, M.; Hyeon, T.; Gruner, S. M.; Wiesner, U. Ordered mesoporous silica nanoparticles with and without embedded iron oxide nanoparticles: structure evolution during synthesis. *J. Mater. Chem.* **2010**, *20* (36), 7807−7814.
(120) Karimi, S.; Heydari, M. Voltammetric mixture analysis of tyrosine and tryptophan using carbon paste electrode modified by newly synthesized mesoporous silica nanoparticles and clustering of variable-partial least square: Efficient strategy for template extraction in mesoporous silica nanoparticle synthesis. *Sens. Actuators, B* **2018**, *257*, 1134−1142.
(121) Zhang, J.; Li, X.; Rosenholm, J. M.; Gu, H.-c. Synthesis and characterization of pore size-tunable magnetic mesoporous silica nanoparticles. *J. Colloid Interface Sci.* **2011**, *361* (1), 16−24.
(122) Chun, B.-S.; Pendleton, P.; Badalyan, A.; Park, S.-Y. Mesoporous silica synthesis in sub- and supercritical carbon dioxide. *Korean J. Chem. Eng.* **2010**, *27* (3), 983−990.
(123) Gunathilake, C.; Jaroniec, M. Mesoporous Organosilica with Amidoxime Groups for CO2 Sorption. *ACS Appl. Mater. Interfaces* **2014**, *6* (15), 13069−13078.
(124) Tsoncheva, T.; Rosenholm, J.; Linden, M.; Ivanova, L.; Minchev, C. Iron and copper oxide modified SBA-15 materials as catalysts in methanol decomposition: Effect of copolymer template removal. *Applied Catalysis A: General* **2007**, *318*, 234−243.
(125) Ji, H.; Fan, Y.; Jin, W.; Chen, C.; Xu, N. Synthesis of Si-MCM-48 membrane by solvent extraction of the surfactant template. *J. Non-Cryst. Solids* **2008**, *354* (18), 2010−2016.
(126) Zhuang, X.; Qian, X.; Lv, J.; Wan, Y. An alternative method to remove PEO−PPO−PEO template in organic−inorganic mesoporous nanocomposites by sulfuric acid extraction. *Appl. Surf. Sci.* **2010**, *256* (17), 5343−5348.

https://doi.org/10.1021/acs.energyfuels.1c04435
Energy Fuels XXXX, XXX, XXX−XXX

(127) Yang, C.-M.; Zibrowius, B.; Schmidt, W.; Schüth, F. Consecutive Generation of Mesopores and Micropores in SBA-15. *Chem. Mater.* **2003**, *15* (20), 3739−3741.
(128) Grudzien, R. M.; Grabicka, B. E.; Jaroniec, M. Effective method for removal of polymeric template from SBA-16 silica combining extraction and temperature-controlled calcination. *J. Mater. Chem.* **2006**, *16* (9), 819−823.
(129) Gai, F.; Zhou, T.; Chu, G.; Li, Y.; Liu, Y.; Huo, Q.; Akhtar, F. Mixed anionic surfactant-templated mesoporous silica nanoparticles for fluorescence detection of Fe3+. *Dalton Transactions* **2016**, *45* (2), 508−514.
(130) Zheng, J.; Tian, X.; Sun, Y.; Lu, D.; Yang, W. pH-sensitive poly(glutamic acid) grafted mesoporous silica nanoparticles for drug delivery. *Int. J. Pharm.* **2013**, *450* (1), 296−303.
(131) Yokoi, T.; Yoshitake, H.; Tatsumi, T. Synthesis of Anionic-Surfactant-Templated Mesoporous Silica Using Organoalkoxysilane-Containing Amino Groups. *Chem. Mater.* **2003**, *15* (24), 4536−4538.
(132) Yokoi, T.; Yoshitake, H.; Tatsumi, T. Synthesis of mesoporous silica by using anionic surfactant. In *Studies in Surface Science and Catalysis*; van Steen, E., Claeys, I. M., Callanan, L. H., Eds.; Elsevier: 2004; Vol. *154*, pp 519−527.
(133) Rahman, N. A.; Widhiana, I.; Juliastuti, S. R.; Setyawan, H. Synthesis of mesoporous silica with controlled pore structure from bagasse ash as a silica source. *Colloids Surf., A* **2015**, *476*, 1−7.
(134) Zhou, Y.; Schattka, J. H.; Antonietti, M. Room-Temperature Ionic Liquids as Template to Monolithic Mesoporous Silica with Wormlike Pores via a Sol−Gel Nanocasting Technique. *Nano Lett.* **2004**, *4* (3), 477−481.
(135) Pérez, L. L.; Ortiz-Iniesta, M. J.; Zhang, Z.; Agirrezabal-Telleria, I.; Santes, M.; Heeres, H. J.; Melián-Cabrera, I. Detemplation of soft mesoporous silica nanoparticles with structural preservation. *Journal of Materials Chemistry A* **2013**, *1* (15), 4747−4753.
(136) Melián-Cabrera, I.; Kapteijn, F.; Moulijn, J. A. Room temperature detemplation of zeolites through H2O2-mediated oxidation. *Chem. Commun.* **2005**, *21*, 2744−2746.
(137) Melián-Cabrera, I.; Kapteijn, F.; Moulijn, J. A. One-pot catalyst preparation: combined detemplating and Fe ion-exchange of BEA through Fenton's chemistry. *Chem. Commun.* **2005**, No. 16, 2178−2180.
(138) Zhang, Z.; Santangelo, D. L.; ten Brink, G.; Kooi, B. J.; Moulijn, J. A.; Melián-Cabrera, I. On the drug adsorption capacity of SBA-15 obtained from various detemplation protocols. *Mater. Lett.* **2014**, *131*, 186−189.
(139) Zhang, Z.; Melián-Cabrera, I. Modifying the Hierarchical Porosity of SBA-15 via Mild-Detemplation Followed by Secondary Treatments. The. *J. Phys. Chem. C* **2014**, *118* (49), 28689−28698.
(140) Kecht, J.; Bein, T. Oxidative removal of template molecules and organic functionalities in mesoporous silica nanoparticles by H2O2 treatment. *Microporous Mesoporous Mater.* **2008**, *116* (1), 123−130.
(141) Yang, L. M.; Wang, Y. J.; Luo, G. S.; Dai, Y. Y. Simultaneous removal of copolymer template from SBA-15 in the crystallization process. *Microporous Mesoporous Mater.* **2005**, *81* (1), 107−114.
(142) Lu, A.-H.; Li, W.-C.; Schmidt, W.; Schüth, F. Low temperature oxidative template removal from SBA-15 using MnO4− solution and carbon replication of the mesoporous silica product. *J. Mater. Chem.* **2006**, *16* (33), 3396−3401.
(143) Hiura, H.; Ebbesen, T. W.; Tanigaki, K. Opening and purification of carbon nanotubes in high yields. *Adv. Mater.* **1995**, *7* (3), 275−276.
(144) Ding, Z.; Chen, J.; Guo, Yu; Xuzhong, G. Study on Removing Organic Template from SBA-15 by HNO3 Oxidation Treatment. *Bulletin of the Chinese Ceramic Society* **2009**, *28*, 80−84.
(145) Wang, Y.; Yang, R. T. Template Removal from SBA-15 by Ionic Liquid for Amine Grafting: Applications to CO2 Capture and Natural Gas Desulfurization. *ACS Sustainable Chem. Eng.* **2020**, *8* (22), 8295−8304.
(146) Ghaedi, H.; Akbari, S.; Zhou, H.; Wang, W.; Zhao, M. Excess Properties of and Simultaneous Effects of Important Parameters on CO2 Solubility in Binary Mixture of Water-Phosphonium Based-Deep Eutectic Solvents: Taguchi Method. *Energy Fuels* **2022**, na DOI: 10.1021/acs.energyfuels.1c03623.
(147) Ghaedi, H.; Kalhor, P.; Zhao, M.; Clough, P. T.; Anthony, E. J.; Fennell, P. S. Potassium carbonate-based ternary transition temperature mixture (deep eutectic analogues) for CO2 absorption: Characterizations and DFT analysis. *Frontiers of Environmental Science & Engineering* **2022**, *16* (7), 92.
(148) Ghaedi, H.; Zhao, M.; Clough, P. T.; Anthony, E. J.; Fennell, P. S. High CO2 absorption in new amine based-transition-temperature mixtures (deep eutectic analogues) and reporting thermal stability, viscosity and surface tension: Response surface methodology (RSM). *J. Mol. Liq.* **2020**, *316*, 113863.
(149) Ghaedi, H.; Zhao, M.; Ayoub, M.; Zahraa, D.; Shariff, A. M.; Inayat, A. Preparation and characterization of amine (N-methyl diethanolamine)-based transition temperature mixtures (deep eutectic analogues solvents). *J. Chem. Thermodyn.* **2019**, *137*, 108−118.
(150) Ghaedi, H.; Ayoub, M.; Sufian, S.; Shariff, A. M.; Lal, B.; Wilfred, C. D. Density and refractive index measurements of transition-temperature mixture (deep eutectic analogues) based on potassium carbonate with dual hydrogen bond donors for CO2 capture. The. *J. Chem. Thermodyn.* **2018**, *118*, 147−158.
(151) Ghaedi, H.; Ayoub, M.; Sufian, S.; Hailegiorgis, S. M.; Murshid, G.; Khan, S. N. Thermal stability analysis, experimental conductivity and pH of phosphonium-based deep eutectic solvents and their prediction by a new empirical equation. *J. Chem. Thermodyn.* **2018**, *116*, 50−60.
(152) Ghaedi, H.; Ayoub, M.; Sufian, S.; Hailegiorgis, S. M.; Murshid, G.; Farrukh, S.; Khan, S. N. Experimental and prediction of volumetric properties of aqueous solution of (allyltriphenylPhosphonium bromide—Triethylene glycol) deep eutectic solvents. *Thermochim. Acta* **2017**, *657*, 123−133.
(153) Ghaedi, H.; Ayoub, M.; Sufian, S.; Shariff, A. M.; Murshid, G.; Hailegiorgis, S. M.; Khan, S. N. Density, excess and limiting properties of (water and deep eutectic solvent) systems at temperatures from 293.15K to 343.15K. *J. Mol. Liq.* **2017**, *248*, 378−390.
(154) Ghaedi, H.; Ayoub, M.; Sufian, S.; Murshid, G.; Farrukh, S.; Shariff, A. M. Investigation of various process parameters on the solubility of carbon dioxide in phosphonium-based deep eutectic solvents and their aqueous mixtures: Experimental and modeling. *International Journal of Greenhouse Gas Control* **2017**, *66*, 147−158.
(155) Ghaedi, H.; Ayoub, M.; Sufian, S.; Hailegiorgis, S. M.; Krishnan, S. Toxicity of Several Potassium Carbonate and Phosphonium-Based Deep Eutectic Solvents towards Escherichia coli and Listeria monocytogenes Bacteria. *J. Environ. Anal Toxicol* **2017**, *7* (485), 2161−0525.
(156) Ghaedi, H.; Ayoub, M.; Sufian, S.; Shariff, A. M.; Lal, B. The study on temperature dependence of viscosity and surface tension of several Phosphonium-based deep eutectic solvents. *J. Mol. Liq.* **2017**, *241*, 500−510.
(157) Ghaedi, H.; Ayoub, M.; Sufian, S.; Lal, B.; Shariff, A. M. Measurement and correlation of physicochemical properties of phosphonium-based deep eutectic solvents at several temperatures (293.15K−343.15K) for CO2 capture. *J. Chem. Thermodyn.* **2017**, *113*, 41−51.
(158) Ghaedi, H.; Ayoub, M.; Sufian, S.; Shariff, A. M.; Hailegiorgis, S. M.; Khan, S. N. CO2 capture with the help of Phosphonium-based deep eutectic solvents. *J. Mol. Liq.* **2017**, *243*, 564−571.
(159) Satlewal, A.; Agrawal, R.; Bhagia, S.; Sangoro, J.; Ragauskas, A. J. Natural deep eutectic solvents for lignocellulosic biomass pretreatment: Recent developments, challenges and novel opportunities. *Biotechnol. Adv.* **2018**, *36*, 2032.
(160) Tan, Y. T.; Chua, A. S. M.; Ngoh, G. C. Deep eutectic solvent for lignocellulosic biomass fractionation and the subsequent conversion to bio-based products − A review. *Bioresour. Technol.* **2020**, *297*, 122522.
(161) Zhang, C.-W.; Xia, S.-Q.; Ma, P.-S. Facile pretreatment of lignocellulosic biomass using deep eutectic solvents. *Bioresour. Technol.* **2016**, *219*, 1−5.